D1-82-0216

"Also available from the author"

BOEING SCIENTIFIC RESEARCH LABORATORIES

Magnetic Fields in the Outer Solar Atmosphere

Ludwig Oster

March 1963

Geo-Astrophysics Laboratory

D1-82-0216

MAGNETIC FIELDS IN THE OUTER SOLAR ATMOSPHERE

by

Ludwig Oster*

Geo-Astrophysics Laboratory

Boeing Scientific Research Laboratories

Seattle 24, Washington

March 1963

*Permanent Address
Yale University Observatory
Box 2023, Yale Station
New Haven, Connecticut

ABSTRACT

On the basis of recent observations, simple mathematical models representing the magnetic field distribution in photospheric layers of the sun are proposed. The structure of the resulting fields in the outer atmosphere and, in particular, the behavior of neutral points is discussed. The expected trapping of charged particles is compared with relevant observations. Several suggestions for further experimental and theoretical studies are advanced.

TABLE OF CONTENTS

LIST OF FIGURES

1. INTRODUCTION

It became increasingly clear in the last several years that the existence of strong magnetic fields in the outer atmosphere of the sun plays a dominant role in the origin and development of disturbances. Unless the mechanism is understood by which these large-scale fields can be produced and maintained, little hope exists for a physically satisfactory explanation of the surprising variety of phenomena summarized in the notion of solar activity. With the increasing interest in space exploration in the years ahead, the strong relationship between the behavior of the interplanetary medium and solar activity becomes even a practically more and more important problem, in particular, since the momentaneous state of the local space environment is one of the factors deciding upon success and failure of some of our space programs.

The at first glance highly irregular occurrence of solar events has rendered so far all precise prediction schemes unsuccessful, in the sense, that, for instance, the onset of a major solar flare cannot be anticipated at a reasonably well defined moment, although there exists a great number of statistical relationships between, say, sunspot number and flare activity. Statistical relations alone, however, are not too helpful in most situations of practical importance.

With the increased emphasis on magnetic fields in the context of solar disturbances, in particular, of solar flares, it is only natural to attempt to correlate features of these fields with certain pecularities of flare events. So far, detailed work has resulted in little progress beyond the basic concepts of magnetogasdynamics. The reasons for this stagnation are two-fold and in neither case easily remedied: firstly, only a limited number of physical processes depend in an observationally useful manner on direction and strength of magnetic fields, thus making it extremely difficult to secure a sufficient variety of observational information on the magnetic field quantities. Secondly, the theoretical relationships combining magnetic field behavior and, in particular, non-thermal processes on the sun are still largely unknown, with the mathematical formalism being prohibitively complex. It was therefore felt that a general re-evaluation of our present-day knowledge might be of some use. Specifically, the several postulated connections between magnetic fields and observed phenomena were thought to offer possibilities for further work (Section 2).

The procedure adopted in this report is then the following: since direct observational evidence for fields is essentially limited to the height levels of the upper photosphere, whereas a number of phenomena occurring in the outer atmosphere is clearly connected in some way or another with the extension of these fields into the

chromosphere and corona (Sections 3 and 4), we attempted to derive simple mathematical models which were adjusted in such a manner that the photospheric observations are satisfactorily represented (Sections 5 and 6). Neutral points, i.e., points in which the total magnetic field strength vanishes, are discussed in Sections 7 and 8. The effects of different pole strengths of leading and following spot in a bipolar group are examined in Section 9. Recent observations of the line-of-sight-component of field strengths in a small group are interpreted in terms of the presented field models (Section 10). Finally, the influence of the coronal plasma itself on the field distribution is discussed in Section 11, with an Appendix in which the formalism for investigating local fields that originate in the corona is presented.

2. FLARES AND MAGNETIC FIELDS

During solar flares, two major non-thermal processes take place: the acceleration of particles to cosmic ray energies, and the emission of electromagnetic radiation exceeding thermal values (i.e. the black body equivalent of the order 10^6°K) by large factors.

It is assumed here that the electromagnetic radiation is a by-product of the production of fast particles, in the sense that the relativistic or nearly relativistic particles during or after acceleration emit the x-rays observed directly as well as indirectly, and that the radio frequency radiation is due to some kind of interaction mechanism with the surrounding corona, yet to be specified.

For the primary process, that is, the acceleration mechanism, electric or magnetic forces could be made responsible on a strictly conceptual basis. However, due to the high conductivity of the solar material, the existence of stationary, large-scale electric fields is virtually impossible, except where strong temperature gradients exist, say, at the transition of chromosphere and corona, and in the neighborhood of prominences. These fields have in principle nothing to do with solar flares.

Hence, the conclusion is that whatever electric fields may be present at the time of a solar flare must be of a type that varies so fast in

time that the accompanying magnetic fields are not negligible. It is then merely a matter of definition whether one attributes the acceleration primarily to the fast varying electric fields or to the magnetic fields.

Taking this concept as the basis for the further discussion, one has to specify the origin of these fast varying fields postulated for the initial state of the flare. "Initial state" stands here in the sense of "at the beginning of the Hα event." The most thorough discussion of this problem is due to Giovanelli (1947, 1948)*, later expanded by Hoyle (1949), although at least the detailed calculations and model assumptions are open to justified criticism; cf. Cowling (1953) and Dungey (1958).

The essential point of Giovanelli's theory is the suggestion that a solar flare comes about by some sort of breakdown, releasing instantaneously a large amount of electromagnetic energy in the form of heat. Severny and co-workers (Severny 1958, 1960; Bumba 1958; Stepanov 1960) have taken up this idea and suggested that some particles in this process reach relativistic energies, high enough to induce thermofusion reactions sustained for enough time to increase further the energy production. A direct verification of this latter conclusion by observing a substantial increase in the intensity of the deuterium lines has so far not produced unambiguous evidence.

---

*References will be found at the end of the text.

In particular, the discharge theory needs the existence of a "neutral point" ("NP") in the magnetic field at which the total magnetic field strength vanishes; cf., for instance, the pictures given by Sweet (1958). A NP appears whenever more than one magnetic pole of a certain sign is present in a group of poles. The existence and position of NP's is therefore a problem whose solution is vital for the interpretation of solar flares. Attempts to predict NP's for a given magnetic field configuration will be discussed in later sections.

Severny has stated that the flares observed in Hα develop around or above NP's. His analysis has been criticized for several reasons. First, the accuracy of magnetic field measurements achieved under normal seeing conditions is usually too poor to allow for detailed magnetic maps. This point has been emphasized by Michard, Mouradian and Semel (1961). Second, the NP's inferred from magnetic maps are guesses, since it is impossible to decide on the basis of the conventional measurements whether a NP is situated in the photosphere or chromosphere, or below the limit of visibility. Third, recent careful measurements of the magnetic field configuration in multipolar spot groups show that flares develop not so much around projected NP's but in regions with predominantly "transverse," that is, horizontal fields, for instance, along the dividing line between N and S poles where no NP's are possible (Bruzek 1958, 1960). Finally, another point of disagreement among observers, however of minor interest for our purposes,

involves the question of whether during a flare event the magnetic field configuration changes drastically. Severny and coworkers (loc. cit.), and Evans (1959) have seen such an effect, but observations by Bruzek (1960), Howard et al. (1959), and Michard et al. (1961) indicate no such change.

It is obvious from the foregoing discussion that a knowledge of the magnetic field configuration in areas and heights where flares are expected is vital for a physical understanding of the flare phenomenon. Lacking observational information, one might attempt to explore on a theoretical basis possible field configurations. Before we go into details in this matter, a discussion of the available evidence for the existence of magnetic fields in the outer atmosphere seems appropriate.

3. MAGNETIC FIELDS IN THE OUTER ATMOSPHERE

The horizontal extent of the magnetic fields of spot groups reaches far beyond the photospheric extent of the group. Evidence to this effect is the formation of long-lived prominences at the outskirts of spot groups later in their development, as shown for instance by a comparison between photospheric magnetic field distributions and prominences (Babcock and Babcock 1958). The cool dense prominence material can only be kept stable in the surrounding hot dilute corona by magnetic fields which prevent a fast decay due to gravitational forces.

The radial extent of the fields can be inferred from the coronal ray structure above sunspots which involves a considerable matter increase in this area. Again, gravitational forces and horizontal diffusion would lead to a fast decay, if no magnetic forces would prevent the outflow of the ionized matter from the region above the spots.

The coronal ray structure is of particular interest, since the direction of magnetic fields can be inferred from the ray structure, if one makes certain assumptions on the coincidence of matter condensations and magnetic fields. An interesting feature in this regard is the often observed inclination of coronal rays against a radius vector from the sun's center which points to an asymmetry in the underlying magnetic field structure. This point will be discussed in detail in a later section.

Another set of observations useful for an estimate of magnetic fields in the outer atmosphere are the radio interferometer data showing the spatial motion (in one or two coordinates) of non-thermal radio sources during and after solar flares. In several instances, this motion clearly deviated from a radial one, suggesting again asymmetries in the magnetic field structure.

Some additional remarks are necessary with respect to the combination of interferometer data and magnetic fields. The underlying concept is that the motion of the source of radiation is

determined by the direction of magnetic fields. In general, two somewhat different theoretical possibilities for the generation of non-thermal radiation are considered, namely, the source being a shock wave, i.e., a disturbance travelling with supersonic speed through essentially stationary material, or a particle cloud travelling as a whole with subsonic speed. In the latter case, the particles clearly have to move along magnetic field lines (that is, in times too small to allow for a substantial particle diffusion across the field lines). Hence, they will move somewhere along the coronal ray structure. However, even for supersonic speeds this statement remains essentially true, since the magnetic stresses will pull the shock wave in a direction parallel to the field, although in the shock front itself the magnetic field lines will of course be deformed; cf. Glasstone and Lovberg (1960).

Once it is established that the fields in the corona result from the particular geometry and strength of photospheric and sub-photospheric fields, one expects a preferred field direction related to the radius vector from the sun's center, but with a statistical distribution of inclinations around it. Since the magnetic field lines determine the path of charged particles such as slow protons, responsible for various phenomena observed in the earth's atmosphere, inclinations in particular cases may

provide a directive effect on the emission of energetic protons. This directivity appears in addition to the general E-W asymmetry of solar proton sources, which has been ascribed to solar rotation (Obayashi and Hakura 1960). Its presence has been recently suggested by Noyes (1962).

4. EXTENSION OF PHOTOSPHERIC FIELDS INTO THE CORONA

Outside of the regions where electric currents flow, the magnetic fields are force-free, i.e.,

$$\nabla \times \vec{H} = 0 \qquad (1)$$

everywhere. Hence, if no currents flow, the atmosphere is in simple hydrostatic equilibrium. Currents, through ohmic heating, will dissipate the mechanical energy into heat, thus pushing the system in time towards the force-free configuration. From the same argument it follows that in steady state the magnetic fields are force-free, at least, for times long compared with a characteristic diffusion time of matter across the field lines. Cowling (1953) points out that in this sense the sunspots' (subphotospheric) fields are clearly not in a steady state. However, it is generally agreed upon that no

appreciable currents flow in the outer atmosphere; cf., Gold (1958) and the discussion by van de Hulst (1958). The argument can be summarized in the sense that the bulk of the current is subphotospheric, whereas a system of small currents of a disturbance nature is required for an understanding of coronal fields.

To first order, the photospheric field structure, due to currents in subphotospheric layers, will then be essentially force-free, with the photospheric fields extending unaltered into the corona and further into interplanetary space. Superimposed on these force-free fields are small additional fields due to local currents in the corona itself. This concept excludes clearly a confinement of the magnetic fields to the photosphere and, maybe, lower chromosphere, with an essentially field-free corona.

Force-free fields at large distance simulate more and more the relatively simple multipole type. This type is clearly not observed in the outer atmosphere with the long outstretched ray structure. The existence of local coronal currents is put into evidence by the increase in density above sunspot groups. In a later section this question will be discussed in more detail. First, however, we shall describe mathematical models for the force-free fields in photospheric layers.

5. MATHEMATICAL MODELS FOR FORCE-FREE FIELDS

On the basis of last section's discussion the following model for the magnetic field distribution is adopted: it is assumed that beneath the photosphere loop currents exist whose centers coincide with longitude and latitude coordinates of visible spots. The height level at which these currents flow is not further specified. The field distribution in the photosphere, and above, is then essentially identical to the field of a solenoid whose one end coincides with the current loop. Since the observed fields are in distant regions, we can bypass a detailed discussion of nature and form of the currents themselves. As a matter of fact, it is of no importance for our applications, whether the current loops are placed at 10,000 or 20,000 km below the photosphere.

Stratton (1941), whose units we transformed into conventional e.s.CGS units, gives the following expressions for the magnetic field components H_ρ and H_z (in cylindrical coordinates) for a circular current loop situated in the ρ-plane ($z = 0$) with the center at the origin:

$$H_\rho = \frac{2I}{C} \cdot \frac{z}{\rho} \left[(a + \rho)^2 + z^2 \right]^{-1/2} \left[-K + \frac{a^2 + \rho^2 + z^2}{(a - \rho)^2 + z^2} E \right], \qquad (2)$$

$$H_z = \frac{2I}{C} \cdot \left[(a + \rho)^2 + z^2 \right]^{-1/2} \left[+K + \frac{a^2 - \rho^2 - z^2}{(a - \rho)^2 + z^2} \; E \right] . \qquad (1)$$

I is the total current, c the velocity of light, a the radius of the current loop. The magnetic susceptibility has been set equal to one everywhere. K and E are the complete elliptic integrals of the first and second kind and of argument

$$k^2 = 4a\rho \cdot \left[(a + \rho)^2 + z^2 \right]^{-1} . \qquad (2)$$

Numerical calculations of the field components for $\rho < a$ and small z have been published by Blewett (1947).

For most of our purposes, the limiting expressions for

$$\rho \gg a, \quad z \gg a \qquad (3)$$

are sufficient (dipole field). They are obtained by expanding k^2, up to quantities of order

$$b^2 = a^2/r^2 , \qquad (4)$$

where

$$r^2 = \rho^2 + z^2 . \qquad (5)$$

We find

$$k^2 = 4b\,\frac{\rho}{r}\left[1 - 2b\cdot\frac{\rho}{r}\right] + O\,(b^3). \tag{8}$$

Similarly

$$\left[(a+\rho)^2 + z^2\right]^{-1/2} = \frac{1}{r}\left\{1 - b\frac{\rho}{r} + b^2\left(\frac{3}{2}\frac{\rho^2}{r^2} - \frac{1}{2}\right) + O\,(b^3)\right\}, \tag{9}$$

$$\frac{a^2+\rho^2+z^2}{(a-\rho)^2+z^2} = 1 + 2b\,\frac{\rho}{r} + b^2\,\frac{4\rho^2}{r^2} + O\,(b^3)\,, \tag{10}$$

$$\frac{a^2-\rho^2-z^2}{(a-\rho)^2+z^2} = -\left\{1 + 2b\,\frac{\rho}{r} + b^2\left[\frac{4\rho^2}{r^2} - 2\right]\right\} + O\,(b^3)\,. \tag{11}$$

Finally, we expand K and E (Dwight 1957):

$$K = \frac{\pi}{2}\left[1 + \frac{1}{4}k^2 + \frac{9}{64}k^4 + O\,(k^6)\right], \tag{12}$$

$$E = \frac{\pi}{2}\left[1 - \frac{1}{4}k^2 - \frac{3}{64}k^4 + O\,(k^6)\right]. \tag{13}$$

Inserting these expressions into Eqs. (2) and (3), the terms $O(b^0)$ and $O(b^1)$ cancel out, and we obtain accurate to $O(b^2)$:

$$H_\rho = \frac{\pi I}{C} \cdot \frac{a^2}{r^5} \cdot 3\rho z \ , \tag{14}$$

$$H_z = \frac{\pi I}{C} \cdot \frac{a^2}{r^5} (2z^2 - \rho^2) \ . \tag{15}$$

The dipole character of the fields (14) and (15) is readily verified by rewriting them in the conventional spherical system of Fig. 1.

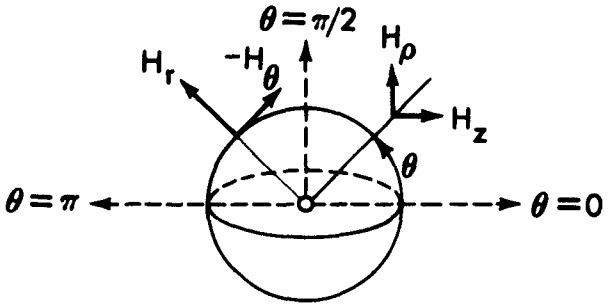

Fig. 1. Spherical coordinate system.

We have

$$z = r \cos \theta, \ \rho = r \sin \theta \ . \tag{16}$$

From the transformations

$$H_r = H_\rho \sin \theta + H_z \cos \theta \ , \tag{17}$$

$$H_\theta = H_\rho \cos \theta - H_z \sin \theta \ , \tag{18}$$

follow

$$H_r = \frac{\pi I}{C} \frac{a^2}{r^3} 2 \cos \theta \tag{19}$$

$$H_\theta = \frac{\pi I}{C} \frac{a^2}{r^3} \cdot \sin \theta \, . \tag{20}$$

Eqs. (19) and (20) describe the field of a magnetic dipole with moment

$$M = \frac{\pi I}{C} a^2 . \tag{21}$$

It is instructive to estimate the order of magnitude of the electric currents required to produce the magnetic fields in the photospheric region. In order to obtain an axial field of

$$H = 10^3 \text{ Gauss} \tag{22}$$

at a distance of

$$r = 10^4 \text{ km} \tag{23}$$

above the plane of the current loop of radius

$$a = 10^3 \text{ km}, \tag{24}$$

a total current

$$I = 10^{24} \text{ e.s. CGS} \tag{25}$$

is required. Letting this current flow in a cylindrical solenoid of thickness

$$d = 100 \text{ km} \tag{26}$$

and height

$$h = 10^4 \text{ km} , \tag{27}$$

a specific current

$$j = 10^8 \text{ e.s. CGS} \tag{28}$$

results. Assuming a velocity of

$$v = 10^3 \text{ km/sec} \tag{29}$$

for the elementary particles responsible for the current, one obtains

$$N = 2 \times 10^9 \text{ cm}^{-3} \tag{30}$$

for the number of electrons (neglecting the slow protons) necessary to maintain the current. Clearly this number is negligible compared with the total number of particles per unit volume in subphotospheric layers.

6. MULTIPOLAR FIELDS

Before we can compare the field model described in the last section with actual observations, we have to work out a few simple relations which hold if more than one current loop (corresponding to one single spot) is present. The aim of this study is to lay the grounds for the explanation of more complex field structures observed in sunspot groups.

We expect no principally new effects from this study, since magnetic fields are strictly additive. Hence all results to be derived follow from simple additions of field structures, taking the respective geometrical conditions into account. Note that a current loop represents magnetically a dipole as shown in the last section, and that therefore an idealized bipolar group has the quadrupole character to be discussed below.

It is worth repeating that the occurrence of a NP in which the total field intensity goes to zero is due to the presence of more than one loop-dipole with the same orientation. Under certain geometrical conditions it is possible that the field configuration degenerates in the sense that the NP's are located at infinity. Such an example is Fig. 2.

The field of two or more current loops in the far-away zone, where the radius vector is large not only compared with the

individual loop radii, but also with the respective distances of the centers of the loops, does not have the familiar dipole character. Simple examples are illustrated in Fig. 2 (linear quadrupole) and Fig. 3 (plane quadrupole). Fig. 4 shows for comparison the dipole field. This dipole field can result in the far-away zone from the combination of four poles as in Fig. 5.

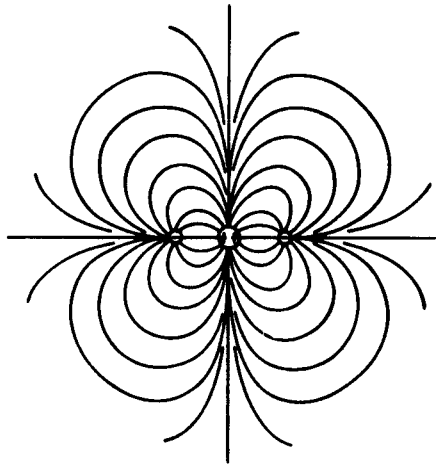

Fig. 2. Linear quadrupole field.

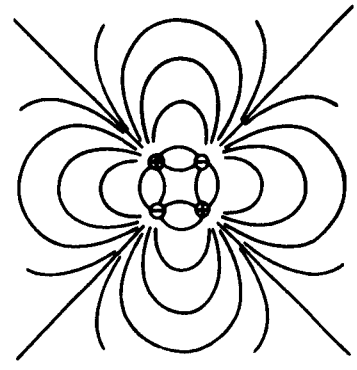

Fig. 3. Plane quadrupole field.

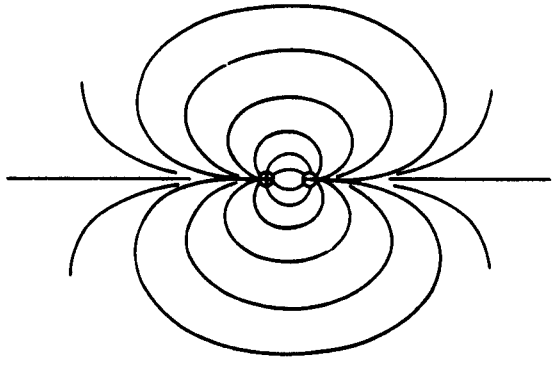

Fig. 4. Dipole field.

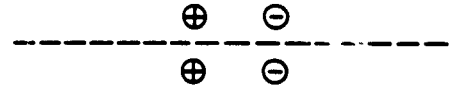

Fig. 5. Four pole configuration which produces a dipole field in the far-away zone.

In the following, simple multipole fields and their properties will be discussed. For our purposes, Eqs. (14) and (15) which hold in the far-away zone of each current loop (dipole fields) are sufficient. The condition

$$k^2 = 4a\rho \left[(a + \rho)^2 + z^2\right]^{-1} \ll 1 \tag{31}$$

effectively places a lower limit on z. For larger values the simplified formulas (14) and (15) may be used irrespective of the relative values of ρ and a.

Since we lose the rotational symmetry by considering more than one current loop at field points whose distances from the centers of the loops are of the same order as the relative distances of the centers, we rewrite Eqs. (14) and (15) in rectangular coordinates:

$$H_x = \frac{\pi I}{C} a^2 \frac{3xz}{r^5} , \tag{32}$$

$$H_y = \frac{\pi I}{C} a^2 \frac{3yz}{r^5} , \tag{33}$$

$$H_z = \frac{\pi I}{C} a^2 \frac{2z^2 - x^2 - y^2}{r^5} \tag{34}$$

where

$$r^2 = x^2 + y^2 + z^2 . \tag{35}$$

Let us first consider the case of two loops lying in the same

plane, say the x-y plane, with their centers on the x-axis at +d and -d. Assume that the absolute values of the currents and the radii are the same for both loops. We then must distinguish between the two possible arrangements of polarities: Case Ia, $\begin{smallmatrix}+ & +\\ - & -\end{smallmatrix}$ and Case Ib, $\begin{smallmatrix}+ & -\\ - & +\end{smallmatrix}$. With the plus sign holding in Case Ia, the minus sign in Case Ib, we have

$$H_x = A \cdot 3z \left\{ \frac{x + d}{r_+^5} \pm \frac{x - d}{r_-^5} \right\} , \tag{36}$$

$$H_y = A \cdot 3zy \left\{ \frac{1}{r_+^5} \pm \frac{1}{r_-^5} \right\} , \tag{37}$$

$$H_z = A \left\{ \frac{2z^2 - y^2 - (x + d)^2}{r_+^5} \pm \frac{2z^2 - y^2 - (x - d)^2}{r_-^5} \right\} , \tag{38}$$

where

$$A = \frac{\pi I}{C} a^2 \tag{39}$$

and

$$r_\pm^2 = (x \pm d)^2 + y^2 + z^2 . \tag{40}$$

In the far-away zone of the quadrupole, that is, for

$$d \ll r_+, r_-; \; r_+ \approx r_- \approx r , \tag{41}$$

Case Ia reduces to the field of a dipole with twice the pole

strength, as already mentioned in connection with Fig. 5.

The interesting case is Ib which reduces to the field of the plane quadrupole (Fig. 3) and is obviously suitable as a model for bipolar groups. The field components read, retaining only terms of order d,

$$H_x = A \cdot \frac{2d}{r^5} \cdot 3z \left[1 - 5\frac{x^2}{r^2} \right], \tag{42}$$

$$H_y = - A\frac{2d}{r^5} \cdot 3z \cdot 5\frac{xy}{r^2}, \tag{43}$$

$$H_z = - A\frac{2d}{r^5} \cdot x \cdot \left[2 + \frac{5}{r^2} (2z^2 - x^2 - y^2) \right]. \tag{44}$$

Note that the quadrupole field varies as r^{-4}, as compared with the r^{-3} variation of the dipole field, Eqs. (14) and (15).

Let us briefly discuss the major features of the quadrupole field (42) - (44), comparing them with the qualitative sketches of Figs. (2) and (3). We specialize for this purpose to the plane of symmetry where y = 0.

The field is purely horizontal ($H_z = 0$) for all values

$$x = 0 \quad \text{or} \quad z = x/2 . \tag{45}$$

On the other hand, the field is vertical ($H_x = 0$) whenever

$$z = 0 \quad \text{or} \quad z = 2x \,. \tag{46}$$

Finally, when

$$z = x \,, \tag{47}$$

we have

$$H_x = H_z = - A\frac{2d}{r^5} \cdot \frac{9}{2}x \,. \tag{48}$$

Fig. 6 shows this behavior in detail for the first quadrant.

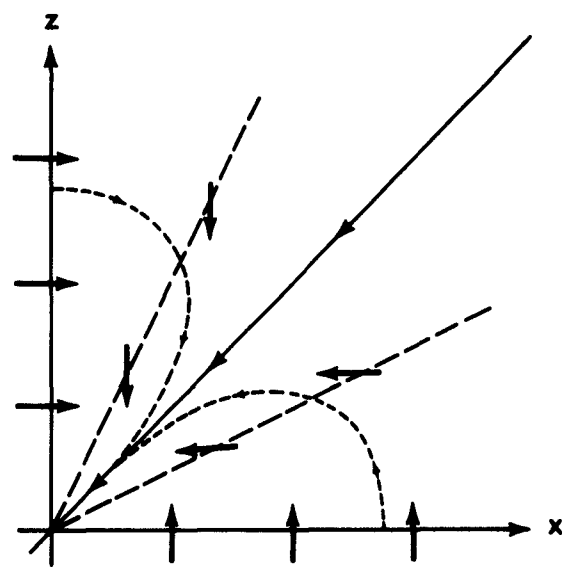

Fig. 6. Field of a plane quadrupole in the first quadrant.

7. NEUTRAL POINTS

Next we discuss some simple cases out of the various possibilities of encountering NP's in multipolar fields, in particular, their relative position and the height variation as a function of typical geometries.

NP's, of course, cannot occur in the far-away zone. Hence, we need the complete expressions of Eqs. (36) - (38) for the quadrupole. The transition to the simplified formulas of the far-away zone places the NP's in the boundary, or inside of the rectangle formed by the four poles.

Consider first the case of the two poles of equal sign situated at $x = d$ and $x = -d$ (case Ia, p. 21), which results in a dipole field at great distance. This case corresponds to two neighboring spots of equal polarity in a complex group. The NP's occur, of course, in the line of symmetry, viz., for

$$x = y = 0; \qquad H_x = H_y = 0 \ . \tag{49}$$

From the conditions on the z - components of the field, viz.,

$$H_z = 2A \frac{2z^2 - d^2}{(z^2 + d^2)^{5/2}} = 0 \ , \tag{50}$$

we find for the height of the NP:

$$z_o = \pm d/\sqrt{2} \ . \tag{51}$$

Next, we compute the field distribution in the y-z plane. For $x = 0$ we still have

$$H_x = 0 \,, \tag{52}$$

whereas

$$H_y = 2A \frac{3zy}{d^2 + y^2 + z^2} \,, \tag{53}$$

$$H_z = 2A \frac{2z^2 - y^2 - d^2}{d^2 + y^2 + z^2} \,. \tag{54}$$

The (horizontal) y-component vanishes only for

$$z = 0 \quad \text{or} \quad y = 0 \,, \tag{55}$$

whereas the (vertical) z-component vanishes along the line given by the relation

$$z^2 = \frac{1}{2} (y^2 + d^2) \,. \tag{56}$$

A graphical representation is given in Fig. 7. Note the NP at the intersection of the curve (56) and the z-axis. Above the curve represented by Eq. (56), the z-field points upwards for a given choice of polarity, below it points downwards.

Second, we consider the linear quadrupole with plus poles situated on the x-axis at $x = +d$ and $x = -d$, the minus pole with relative strength n at $x = 0$. This case is realized, for

instance, if midway between leading and following spot in a bipolar group a third spot is found. Specializing again to the plane of symmetry y = 0 we find

$$H_x = A \cdot 3z\left\{\frac{x+d}{r_+^5} - n\frac{x}{r^5} + \frac{x-d}{r_-^5}\right\}, \tag{57}$$

$$H_y = 0, \tag{58}$$

$$H_z = A\left\{\frac{2z^2-(x+d)^2}{r_+^5} - n\frac{2z^2-x^2}{r^5} + \frac{2z^2-(x-d)^2}{r_-^5}\right\}. \tag{59}$$

In the line of symmetry x = 0, and

$$H_x = 0, \tag{60}$$

$$H_z = A\left\{2\frac{2z^2-d^2}{(z^2+d^2)^{5/2}} - \frac{2n}{z^3}\right\}. \tag{61}$$

The condition for vanishing vertical field, $H_z = 0$, can be written in the form

$$n^2 = p^6\frac{(2p^2-1)^2}{(p^2+1)^5}, \tag{62}$$

where

$$p = z/d. \tag{63}$$

The solution of Eq. (62) must be found by numerical methods. We have plotted in Fig. 8 the right hand side of Eq. (62). The intersection with the lines n^2 = [right hand side of (62)]

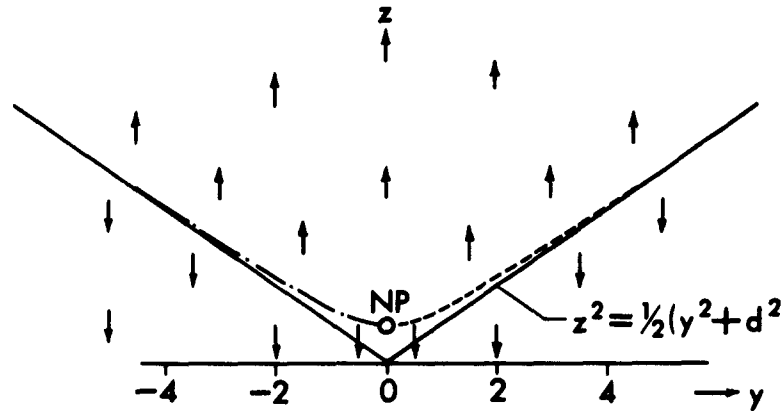

Fig. 7. Neutral point in the y-z plane due to two equal poles at x = +d and -d.

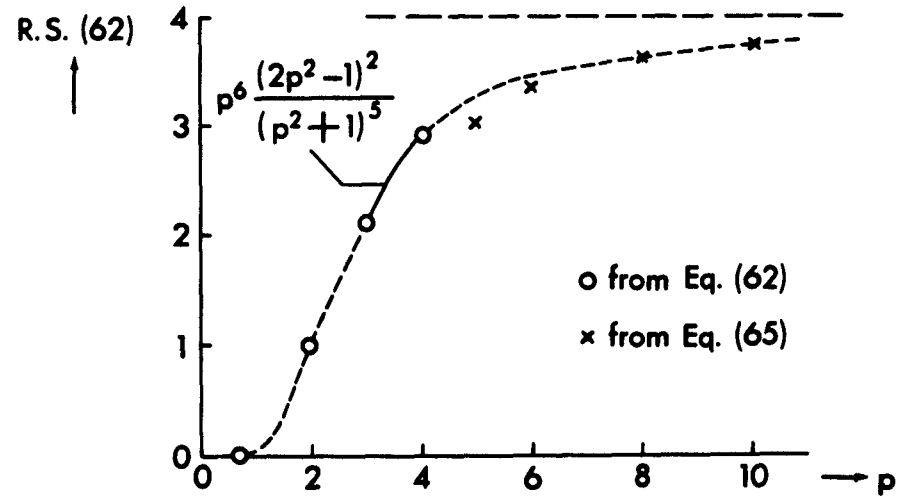

Fig. 8. The function $p^6 \frac{(2p^2 - 1)^2}{(p^2 + 1)^5}$ of Equation (62).

gives the heights of the NP's. For values

$$p \gg 1 \tag{64}$$

Eq. (62) becomes approximately

$$n^2 = 4\left(1 - \frac{6}{p^2}\right) . \tag{65}$$

The height behavior of the neutral points is very interesting. For n = 1, the height equals almost exactly twice the half distance between the two outer poles. Increasing the strength of the middle pole moves the NP further and further up, until for n = 2 (linear quadrupole in the strict sense) the NP is at infinity. No NP occurs for $n^2 > 4$ in the upper half plane.

For n < 1, the height of the NP decreases further, reading zero for n = 0, where the intersection points

$$p = z = 0 \quad \text{and} \quad z = d/\sqrt{2} \tag{66}$$

lead back to Eq. (51).

Finally, let us consider the combination of two plane quadrupoles. There are two extreme cases, which are of interest with regard to sunspots. First, assume that the centers of the quadrupoles are on the x-axis at x = D and x = -D, and that their planes coincide. Such a system is realized by two spot groups at the same latitude, their distance being 2D.

Furthermore, let

$$D \gg d, \tag{67}$$

but not necessarily

$$D \gg r, \tag{68}$$

so that we might use the formulas for the far-away zone of each quadrupole, but retain the complete expression as far as their combination is concerned.

For the discussion of NP's, we need the x - component of the field which reads

$$H_x = 6Adz \left\{ \left[\frac{1}{r_-^5} - 5\frac{(x - D)^2}{r_-^7} \right] \pm \left[\frac{1}{r_+^5} - 5\frac{(x + D)^2}{r_+^7} \right] \right\} \tag{69}$$

where

$$r_\pm^2 = (x \pm D)^2 + y^2 + z^2 \ . \tag{70}$$

The plus sign combining the two expressions in the main bracket of Eq. (69) applies to the combination of polarities of Fig. 9 (Case IIa). The minus sign, corresponding to the combination of polarities of Fig. 10 (Case IIb), is of less interest for solar applications.

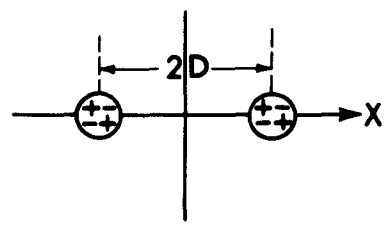

Fig. 9. Configuration of quadrupoles on x-axis, Case IIa.

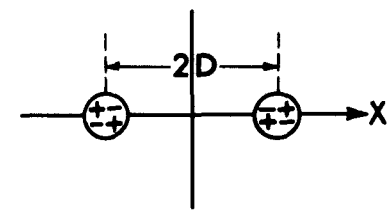

Fig. 10. Configuration of quadrupoles on x-axis, Case IIb.

In the symmetry axis x = y = 0,

$$H_x = 6Adz \left[\frac{z^2 - 4D^2}{z^2 + D^2} \pm \frac{z^2 - 4D^2}{z^2 + D^2} \right] . \tag{71}$$

In Case IIb, H_x is identically zero for all values of z, i.e., no NP occurs. However, in Case IIa we have a neutral point at

$$z = 2D \ . \tag{72}$$

H_z vanishes for all z-values.

Second, consider an arrangement of two quadrupoles on the y-axis at +D and -D, with the planes of symmetry parallel between themselves and to the x-axis (Figs. 11 and 12). The combination may serve as a model for two groups situated at the same longitude, but on opposite hemispheres. This geometry does not lead to any NP along the z-axis in the sense we used the term NP previously, whatever the arrangement of polarities may be. To see this point, we recall from Eqs. (43) and (44) that

$$H_y = H_z = 0, \qquad \text{if} \qquad x = 0 \tag{73}$$

Furthermore,

$$H_x = 6Adz \left\{ \left[z^2 + (y + D)^2 \right]^{-5/2} \pm \left[z^2 + (y - D)^2 \right]^{-5/2} \right\} . \tag{74}$$

For y = 0, the case of Fig. 11 leads to the condition

$$(z^2 + D^2)^{-1} = 0 \tag{75}$$

(no NP for finite z-values), whereas in the case of Fig. 12

$$H_x = H_y = H_z = 0 \tag{76}$$

along the whole z-axis.

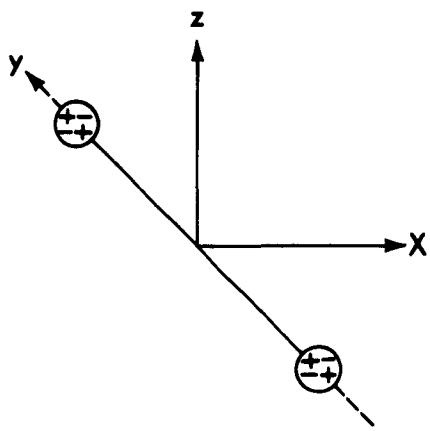

Fig. 11. Configuration of quadrupoles on y-axis.

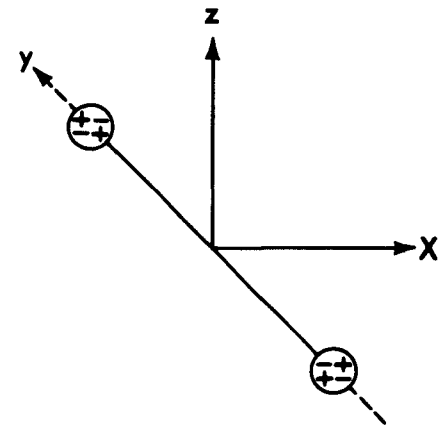

Fig. 12. Configuration of quadrupoles on y-axis.

To probe a little further into this interesting field geometry, we quote the field components in the midplane y = 0:

$$H_y = 60AdD \frac{zx}{(x^2 + D^2 + z^2)^{7/2}} , \tag{77}$$

$$H_x = H_z = 0 . \tag{78}$$

Eqs. (77) and (78) show that the field everywhere in the midplane is horizontal, and that it reverses sign at x = 0 in the

manner illustrated in Fig. 13.

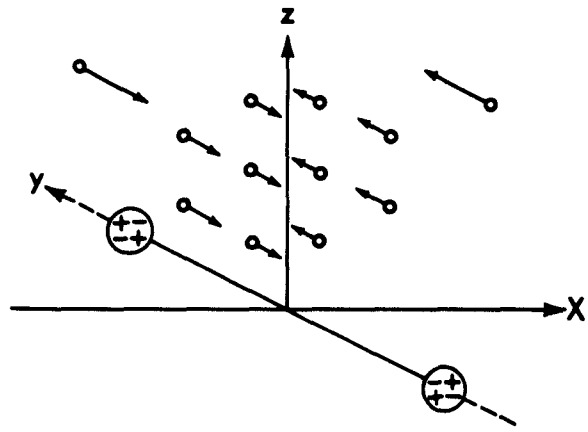

Fig. 13. Field in quadrupole midplane.

The simple model calculations presented in this section may be used in predicting field geometries above sunspots and groups. First we conclude that NP's within the boundaries of one group can only occur between spots of equal polarity (Case Ia, p.21), with the height roughly equal to half the distance between the poles, corresponding thus to photospheric layers. Adding a pole of opposite polarity in the symmetry point lifts the NP up depending on the relative pole strength. This result points to the fact that the height behavior of NP's strongly depends on the specific geometrical conditions between spots in a group. This question will therefore be discussed somewhat further in the next section.

The computations for the combination of two plane quadrupoles

can be used either for complex groups or, in particular, for the combined field of different groups. We conclude from Eq. (72) that the height of the NP (if there is a NP at all; cf. Eq. (71)) is approximately equal to the distance between the two centers of the quadrupoles. For two groups on the same hemisphere, any NP will therefore be far up in the corona.

The mathematical basis for a detailed discussion of the fields of two groups on different hemispheres would have to start from the geometry of Fig. 12. where we find along the whole symmetry axis zero total field. In the mid plane, corresponding to the equatorial plane of the sun, the field is uniformly horizontal, however, changing sign on passing through the meridian connecting the two groups.

8. HEIGHT BEHAVIOR OF NEUTRAL POINTS IN COMPLEX FIELD STRUCTURES

The results of the last section indicate that height and position of NP's are critically dependent on the geometry of poles in complex groups. To study this behavior a little further, we begin by discussing the relatively simple case of two poles of equal

polarity situated on the x-axis at ±d. This system of poles generates a NP at $z = d/\sqrt{2}$. Add another pole at $x = D$ with a ratio n of pole strengths ($n \gtrless 0$). The z - component of the field then reads ($x = y = 0$):

$$H_z = A\left\{\frac{2z^2 - d^2}{(z^2 + d^2)5/2} + n\frac{2z^2 - D^2}{(z^2 + D^2)5/2}\right\}. \tag{79}$$

The first term alone (Eq. (51)) leads to a NP at

$$z = z_o = d/\sqrt{2}, \tag{80}$$

as already mentioned. The second term alone, of course, does not lead to a NP, since it represents the field in the far-away zone of one single pole. However, the z-component changes sign at

$$z = D_o = D/\sqrt{2}. \tag{81}$$

The case of interest for our purposes requires

$$D_o > z_o, \tag{82}$$

since the contribution H_z^I to the z-component of the total field from the first term in Eq. (79) for $n > 0$,

$$H_z^I > 0, \qquad \text{if} \qquad z > z_o, \tag{83}$$

$$< 0, \qquad z < z_o, \tag{84}$$

whereas the contribution from the second term,

$$H_z^{II}(z = z_o) < 0. \tag{85}$$

The effective height of the NP is <u>increased</u> if $n > 0$. Reversing the polarity ($n<0$) of the added pole in Eq. (79), <u>lowers</u> the NP.

However, the computation so far does not refer to a true NP, because for $z = z_o$

$$H_x^{II} = 3nAD \frac{z_o}{(z_o^2 + D^2)^{5/2}} \quad . \qquad (\text{illegible})$$

In fact, the true NP shifts not only in height (z-coordinate), but also along the x-axis. In order to find this variation, we need the expression corresponding to Eq. (79) for the x-component of the field. We still retain $y = 0$, but now have to consider finite values of x:

$$H_x = 3zA \left\{ \frac{x + d}{\left[(x + d)^2 + z^2\right]^{5/2}} + \frac{x - d}{\left[(x - d)^2 + z^2\right]^{5/2}} + n \frac{x - D}{\left[(x - D)^2 + z^2\right]^{5/2}} \right\} . \qquad (8$$

For the qualitative discussion to follow, the simplifying condition

$$x \ll d \qquad (8$$

may be used which effectively places a certain upper limit on the combination $n\, D^{-3}$ (cf. Eq. (90)).

Expanding the first two terms of Eq. (87) and taking (88) into account, we obtain

$$H_x^I = \frac{6zxA}{(d^2 + z^2)^{5/2}} \left[1 - \frac{10d^2}{d^2 + z^2}\right] \approx - \frac{8.17}{9\cdot\sqrt{3}} \cdot \frac{x}{d^4} A \, . \qquad (8$$

On the other hand,

$$H_x^{II} \approx -3AnD^{-3}z, \tag{90}$$

Hence, from the condition

$$H_x^I + H_x^{II} = 0 \tag{91}$$

we see that a third positive pole at x = D (n>0) will push the NP away and up, an opposite pole (n<0) will push the NP closer and down (Figs. 14 and 15)

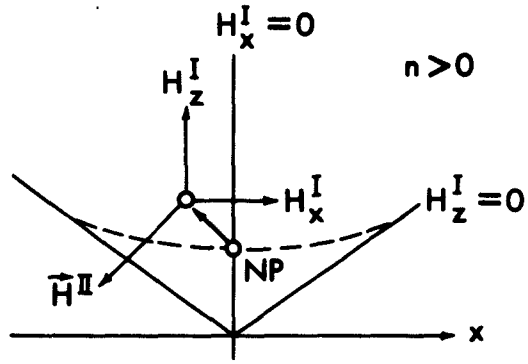

Fig. 14. Neutral point for unit poles at x = ±d and pole of strength n(>0) at D.

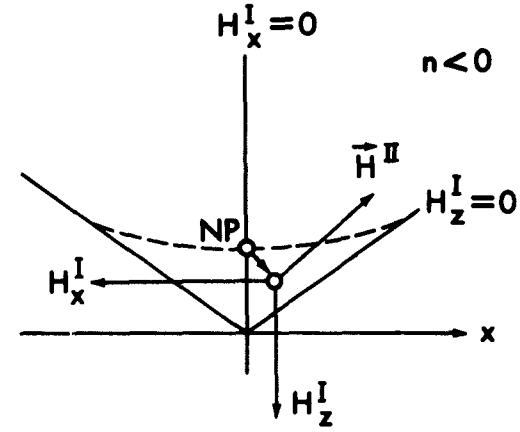

Fig. 15. Neutral point for unit poles at x = ±d and pole of strength n(<0) at D.

The sign of H_x^I might seem strange at first sight. In fact, H_x^I changes sign when

$$z = 3d \tag{92}$$

A closer inspection of the field lines around the NP and above

reveals, however, that this behavior is well to be expected. For details see the illustration in Fig. 16.

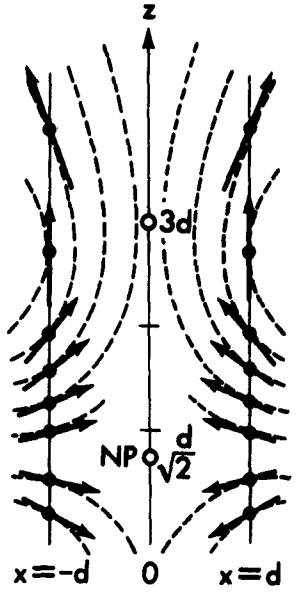

Fig. 16. Details of H_x for two equal poles at $x = \pm d$.

We now turn to the case where the third pole is situated on the y-axis, i.e., at right angle to the plane of the quadrupole, at $y = D$, while the two poles are placed as before at $x = d$ and $x = -d$. We recall from Eq. (56) and, in particular, from Fig. 7 that

$$H_z^I = 0, \qquad \text{if} \qquad z = \frac{1}{\sqrt{2}} (y^2 + d^2)^{1/2} . \tag{93}$$

As contribution from the third pole we have

$$H_z^{II} = nA \frac{2z^2 - x^2 - (y - D)^2}{\left[x^2 + (y - D)^2 + z^2\right]^{5/2}} . \tag{94}$$

In particular, for $x = 0$,

$$H_z^{II} = 0, \qquad \text{if} \qquad z = \frac{1}{\sqrt{2}} (y - D) . \tag{95}$$

Both conditions (93) and (95) are satisfied for

$$y' = \frac{D^2 - d^2}{2D} , \tag{96}$$

with the corresponding height coordinate

$$z' = \frac{1}{\sqrt{2}} \frac{D^2 + d^2}{2D} , \tag{97}$$

At $y = y'$, the y-component of the field will not vanish in general ($H_x = 0$, of course). The somewhat tiresome calculation leads to the result that

$$H_y (y = y') = 0 \qquad \text{only if} \qquad D^2 = 3 d^2 , \tag{98}$$

i.e., a true NP will only exist in a very special geometrical arrangement of poles.

So far, our analysis has not been the most general one. As a matter of fact, it is possible that a true NP exists because the contributions I and II cancel each other, but do not vanish separately. The existence of such a point is not trivial. Since its existence may possibly be of importance for the occurrence of flares, it seems worthwhile to expand the preceding analysis a step further.

The general equations for the geometry under consideration are

$$H_x = A \cdot 3\,(x + d)\,\frac{z}{r_+^5} + A \cdot 3\,(x - d)\,\frac{z}{r_-^5} + nA\,\frac{3xz}{r_D^5}\,, \tag{99}$$

$$H_y = A\,\frac{3yz}{r_+^5} + A\,\frac{3yz}{r_-^5} + nA\,\frac{3\,(y - D)z}{r_D^5} \tag{100}$$

$$H_z = A\,\frac{2z^2 - (x + d)^2 - y^2}{r_+^5} + A\,\frac{2z^2 - (x - d)^2 - y^2}{r_-^5}$$

$$+ nA\,\frac{2z^2 - x^2 - (y - D)^2}{r_D^5}\,, \tag{101}$$

where

$$r_\pm^5 = \left[(x \pm d)^2 + y^2 + z^2\right]^{5/2};\quad r_D^5 = \left[x^2 + (y - D)^2 + z^2\right]^{5/2}. \tag{102}$$

The problem is to find a point (x_o, y_o, z_o) for which all three field components vanish. Clearly, H_x vanishes only for

$$x = 0, \tag{103}$$

disregarding the solution $z = 0$ which is of no interest to us. Condition (103) has already been used in the simplified analysis of pp. 37 and 38.

Eqs. (100) and (101) reduce to

$$0 = \frac{2y}{(d^2 + y^2 + z^2)^{5/2}} + n\,\frac{y - D}{\left[(y - D)^2 + z^2\right]^{5/2}}\,, \tag{104}$$

$$0 = 2\,\frac{2z^2 - d^2 - y^2}{(d^2 + y^2 + z^2)^{5/2}} + n\,\frac{2z^2 - (y - D)^2}{\left[(y - D)^2 + z^2\right]^{5/2}} \quad . \tag{105}$$

It is clear that in general the solution $(0, y_o, z_o)$ must be found by numerical means. It is equally clear that the existence of a physically interesting solution (y_o, z_o real, positive, etc.) depends entirely on the field constants d, D and n. Recalling the often very complex space distribution of spots of different polarities in a group, and the fact that NP's must lie in a very limited range of heights corresponding to chromospheric altitudes, if they are in any way responsible for the onset of flares, it is safe to conclude that all these conditions are hardly satisfied in a wide majority of cases. It is interesting to think that the occurrence of a flare might be connected with the appearance of a NP at the "right" altitude during the slow changes of spot fields.

Without going into numerical calculations, we conclude this discussion by deriving limiting expressions for the system of Eqs. (104) and (105). First, after some algebra, one obtains the alternate set

$$z^2 = -\frac{1}{2}y^2 + \frac{y}{2D}(D^2 - d^2) + \frac{d^2}{2} \quad , \tag{106}$$

$$\left[\frac{(y - D)^2 + z^2}{y^2 + d^2 + z^2}\right]^{5/2} = n \cdot \frac{D - y}{2y} \quad . \tag{107}$$

Assume that

$$D >> d,\ y_o,\ z_o\ . \tag{108}$$

The inequalities (108) are legitimate, since for

$$D \to \infty : z \to z_o = d/\sqrt{2};\ y_o \to 0\ . \tag{109}$$

Define

$$y_o = \delta\ ,\quad z_o = \frac{1}{\sqrt{2}}\, d + \varepsilon\ , \tag{110}$$

and neglect terms of order 2 and higher in δ and ε. If finally

$$\delta^2 << d\,\varepsilon\ , \tag{111}$$

we obtain

$$y_o = \delta = \frac{3d}{4}\sqrt{6}\ n\left(\frac{d}{D}\right)^4 \tag{112}$$

and

$$z_o = \frac{d}{\sqrt{2}}\left[1 + \frac{3}{8}\sqrt{6}\ n\left(\frac{d}{D}\right)^3\right]. \tag{113}$$

The inequality (111) is now readily verified. In addition, we find that a fortiori

$$\varepsilon >> \delta\ . \tag{114}$$

The discussion can be summarized by stating that the height of the NP is increased by adding the positive pole, decreased

by an additional negative pole. The situation is analogous to the case of a perturber in line with the two main poles (p. 36, Figs. 14 and 15). The horizontal shift, however, is just opposite: the additional pole will attract the NP if it is of the same sign, and push the NP away if the signs of the pole combinations are opposite. Finally, the shift in height greatly outweighs the horizontal shift.

9. EFFECTS OF DIFFERENT MAXIMUM POLE STRENGTHS IN BIPOLAR GROUPS

It was mentioned in Section 3 that in addition to the EW-asymmetry due to the solar rotation the influx of solar protons at the earth may reveal an asymmetry in the original emission angle (Noyes 1962). One possible reason for such an effect would be a difference in pole strength of positive and negative polarities of bipolar groups. In order to obtain a qualitative picture of the implications of this suggestion, we take the model case where a positive pole of strength one in arbitrary units is placed at $x = -d$, a negative pole strength $-n$ is placed at $x = +d$. The z-component of the field then reads (Eq. 38) in the plane $y = 0$:

$$H_z = (1 - n) \frac{A}{r^5} \left[2z^2 - x^2 - d^2 - 2 \frac{1 + n}{1 - n} dx \right] , \qquad (115)$$

where we have replaced r_+ and r_- (Eq. 40) in the denominator by

$$r^2 = x^2 + z^2 \ . \tag{116}$$

Again, this combination of poles in the far-away zone does not approach a dipole field, as can be seen, for instance, in the value of the x-coordinate at which H_z vanishes:

$$x_o = \frac{1 + n}{1 - n} d \pm \left[\frac{2n}{(1 - n)^2} d^2 + 2z^2 \right]^{1/2} \ . \tag{117}$$

If

$$z^2 >> \frac{n}{(1 - n)^2} d^2 \ , \tag{118}$$

we have simply

$$x_o = \pm \sqrt{2}\, z \ . \tag{119}$$

This result is remarkable for several reasons. The locations x_o of the abscissa corresponding to $H_z = 0$ are symmetric with respect to the axis of the quadrupole. The angle between the lines of vanishing z-component is

$$2 \tan^{-1} \sqrt{2} \approx 110^\circ \ . \tag{120}$$

This angle is independent of the relative pole strength n. The effect seems surprising at first, since for $n = 1$ we know from Eq. (48) that $x_o = 0$. We note however, that in this case the present analysis breaks down, since then Eq. (118) requires an infinite z-value. In fact, the closer n comes to unity, the

further out in z-direction we have to go before we can apply the asymptotic formula (119).

H_z does not vanish for $x = 0$. If

$$z^2 >> d^2 , \tag{121}$$

a condition considerably weaker than (118),

$$H_z \approx \frac{2A}{z^3}(1 - n) . \tag{122}$$

Hence, for $n < 0$, H_z is positive; for $n > 0$, it is negative. A schematic picture of the field lines is drawn in Fig. 17.

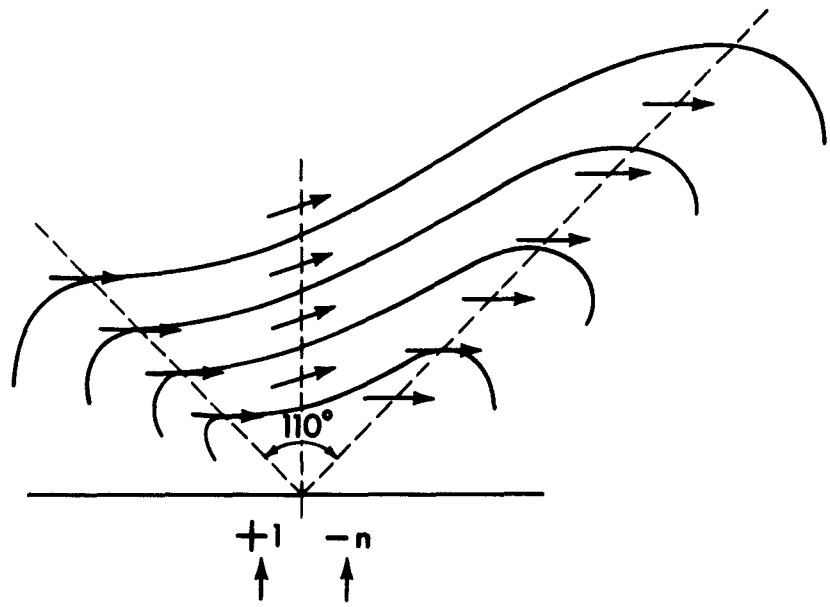

Fig. 17. Field for poles of strength +1 and -n at $x = -d$ and $x = +d$ respectively.

Mathematically, the analysis carried out so far corresponds to replacing the hyperbola

$$(x_o + \frac{1 + n}{1 - n}d)^2 - 2z^2 = \frac{4n}{(1 - n)^2} d^2 , \tag{123}$$

which is the exact location of the points of vanishing H_z, by its asymptotes (119). The net effect of the inequality of pole strengths ($n \neq 1$) is to bend the field lines in such a way that the axis along which the field is horizontal and reaches further out, is inclined to the normal and towards the weaker pole. For heights below the critical value (118) the inclination is less, going to zero as z approaches 0. The inclination at large distances becomes independent of the absolute value of n; however, the characteristic heights at which the inclination has reached a certain percentage of its asymptotic value depend on n. The general behavior is schematized in Fig. 18.

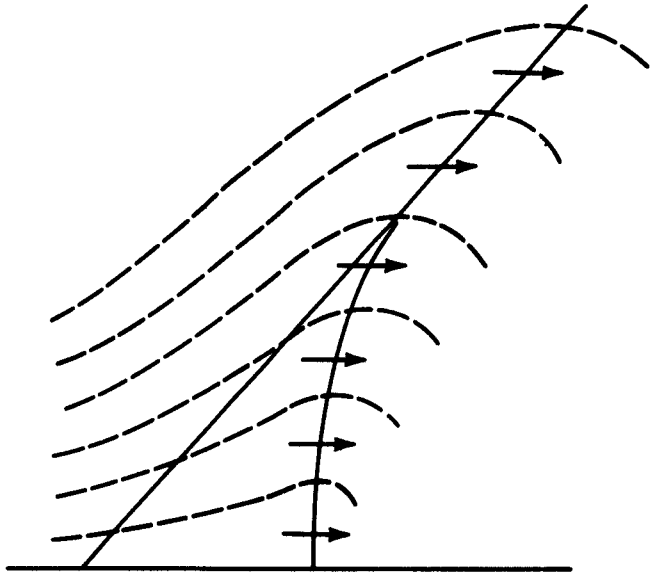

Fig. 18. Inclination of line along which field is horizontal, for the case of two poles of unequal strength.

In concluding, we investigate the characteristic distances involved in (118) for typical conditions on the sun, postulating that

$$z^2 \geq z_o^2 = 100 \frac{n}{(1-n)^2} d^2 \quad . \tag{124}$$

For a typical sunspot group,

$$d = 10^4 \text{ km}, \quad z_o \approx \begin{cases} 10^6 \text{ km} \approx 1.5\ R_o \\ \\ 90{,}000 \text{ km} \end{cases} \quad \text{for} \quad n = \begin{cases} .90 \\ \\ .33 \end{cases} . \tag{125}$$

Grotrian and Künzel (1950) concluded from a statistical analysis that the magnetic flux of the preceding spots of a bipolar group is on the average three times the flux of the following spots. However, considering all the difficulties in obtaining accurate measurements of maximum field strengths and spot areas at the same time, this value can only mean an estimate of orders of magnitude.

Whatever the average value of n is, coronal rays and particle paths will tend to be inclined towards the east on the sun, reaching about 55° from the normal at larger distances. The effect is in the same direction as the bending of field lines due to the solar rotation, if it is assumed that this rotation is not rigid in interplanetary space. In addition, an EW-asymmetry in the projected positions of sources in the corona follows, in the

sense, that more sources should be observed east of the central meridian, but only if identified with active regions on the surface. The total amount of coronal sources is, of course, not affected by this inclination.

At any rate, whatever the net effects of this inclination on terrestrial events may be, any such asymmetry would depend on the degree of asymmetry in the magnetic field structure of underlying spot groups.

At present not enough material is available to corroborate this suggestion by statistical data. Once more observations are made, such a study may be of some value.

10. DISCUSSION OF PHOTOSPHERIC OBSERVATIONS

In the following sections, a few applications of the field models are discussed which might be suitable for observational tests. Admittedly, the suggestions to be advanced are rather sketchy; however, it is felt that progress along these lines could be made later. The purpose of this discussion is therefore not so much to arrive at specific results, but to demonstrate the possibilities an expanded analysis on the basis of more material might present. We begin by discussing a typical case of photospheric observations.

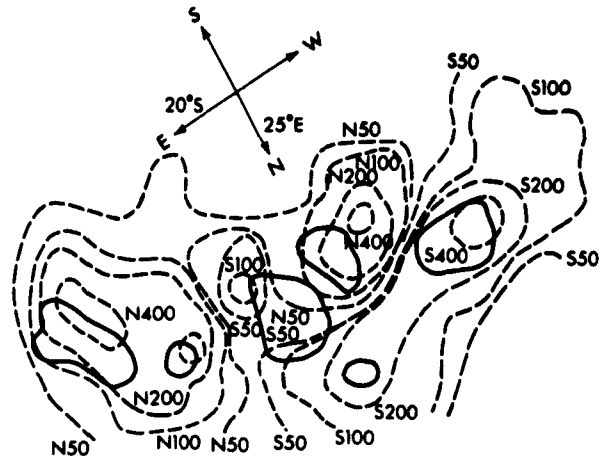

Fig. 19. Isogauss contours in a spot region (Michard et al., 1961).

Accurate observations of the magnetic field distribution in sunspot groups are still scarace. We have chosen as a test example of how our ideas can be applied to the interpretation of observed field structures, the small spot group described in detail by Michard et. al., (1961). In Fig. 19 the essential features are summarized. The solid lines are the photographically observed penumbra rims of the sunspots, the dashed lines are isogauss lines corresponding to 50, 100, 200 and 400 Gauss. Points of later interest are identified in Fig. 20. The quoted numerical values correspond to field components in the line of sight, i.e., the direction connecting the photospheric location and the observer on the earth.

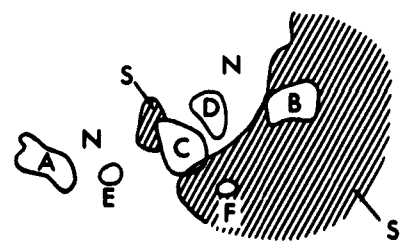

Fig. 20. Identification of points of interest in Figure 19.

The following observations should be explained:

(1) The maximum field strengths are shifted towards the west as compared with the white-light observations.

(2) The amount of shift differs characteristically for the spots A and B on one side, for C and D on the other side. The scale is such that the distance between the two extreme spots is about 5°3 on the sun.

(3) The double N-poles corresponding to A and E, and the two S-poles corresponding to B and F show separate maxima, whereas the (strongly) shifted maximum corresponding to the two N-spots C and D is single.

(4) There is a S-pole region in the neighborhood of spot C ("enclave de polarité S anormale"). Its strength is considerably less than the maxima connected with A or B.

Before we discuss these details we should like to cite the authors, saying that the isogauss lines as well as the spot areas carry considerable observational error, due to the intrinsic difficulties of magnetic field measurements, and to the rather inferior seeing conditions on that date (23 April 1960). In the spot group a flare of importance 1 or 1+ developed, and Michard et al., found that no change in the field configuration outside of statistical fluctuations due to seeing conditions occurred. The authors emphasize that this criticism against their own work applies as well to all other field measurements, which very often report minute details that may well be spurious. We may guess that relative spot

positions are uncertain by about the spot's diameter, with at least the same error for the isogauss lines.

Summarizing the discussion to follow we state that

(1) the shift of the field maxima with respect to the photospheric spot locations is due to the angle between the line of sight and the radial direction on the sun; that

(2) the difference in amount is caused by the fact that (C+D) is affected differently than the essentially single poles A and E, or B and F; that

(3) the appearance of A and E as single poles is due to the greater relative distance between A and E as compared with C and D, and/or possibly to a difference in height of the locations of generating current loops; that

(4) the appearance of a S-pole between E+A and C+D reflects the fact that the level in which the major portion of the spectral line used by Michard et al., corresponds to a height below the NP generated by the two quadrupoles A+E and C+D, whereas the corresponding NP's for A and E, C and D, and B and F are all below this level.

The fact that the magnetic field measured at the location of the (N-pole) spot C is S-polar is then readily explained by the very nature of the measurements. The intrinsic observational uncertainties, however, make it not worthwhile to discuss in detail the mutual influences of, say, the spots A, C, D, E on the NP between B and F. We therefore restrict our considerations to a qualitative

analysis, giving numerical illustrations as we go along.

In order to verify the above statements we first quote Eq. (51) which shows a linear dependence of the height z_o of the NP on the distance d between two spots of equal polarity. This is the basis of points (3) and (4).

In Fig. 21, H_z/A is plotted as a typical example for the combination of two plus poles at x = 5 and x = -5, and for a height z = 2. The appropriate formula is Eq. (38) with the positive sign; the NP would be situated at z≈3.5. Note that the maximum intensity of the negative field between the poles is only about 2 percent of the positive field strength above the poles.

The opposite case, $z > z_o$, is illustrated in Fig. 22 for z = 12.5 and the same position of the poles. For comparison, a single pole with the same strength as one of the others and situated at x = 0 is plotted in Fig. 23. Note that the maximum intensity of the two poles (5.21×10^{-4} units) is only slightly above the maximum of the intensity of a single pole (4.09×10^{-4} units).

Finally, we check the behavior of the maxima as a function of x(y=0). Differentiating Eq.(38) with respect to x results in

$$\frac{\partial H_z}{\partial x} = 0 = -2(x + d) - 5(x + d)\frac{2z^2 - (x + d)^2}{z^2 + (x + d)^2} - 2(x - d) - 5(x - d)\frac{2z^2 - (x - d)^2}{z^2 + (x - d)^2}. \qquad (126)$$

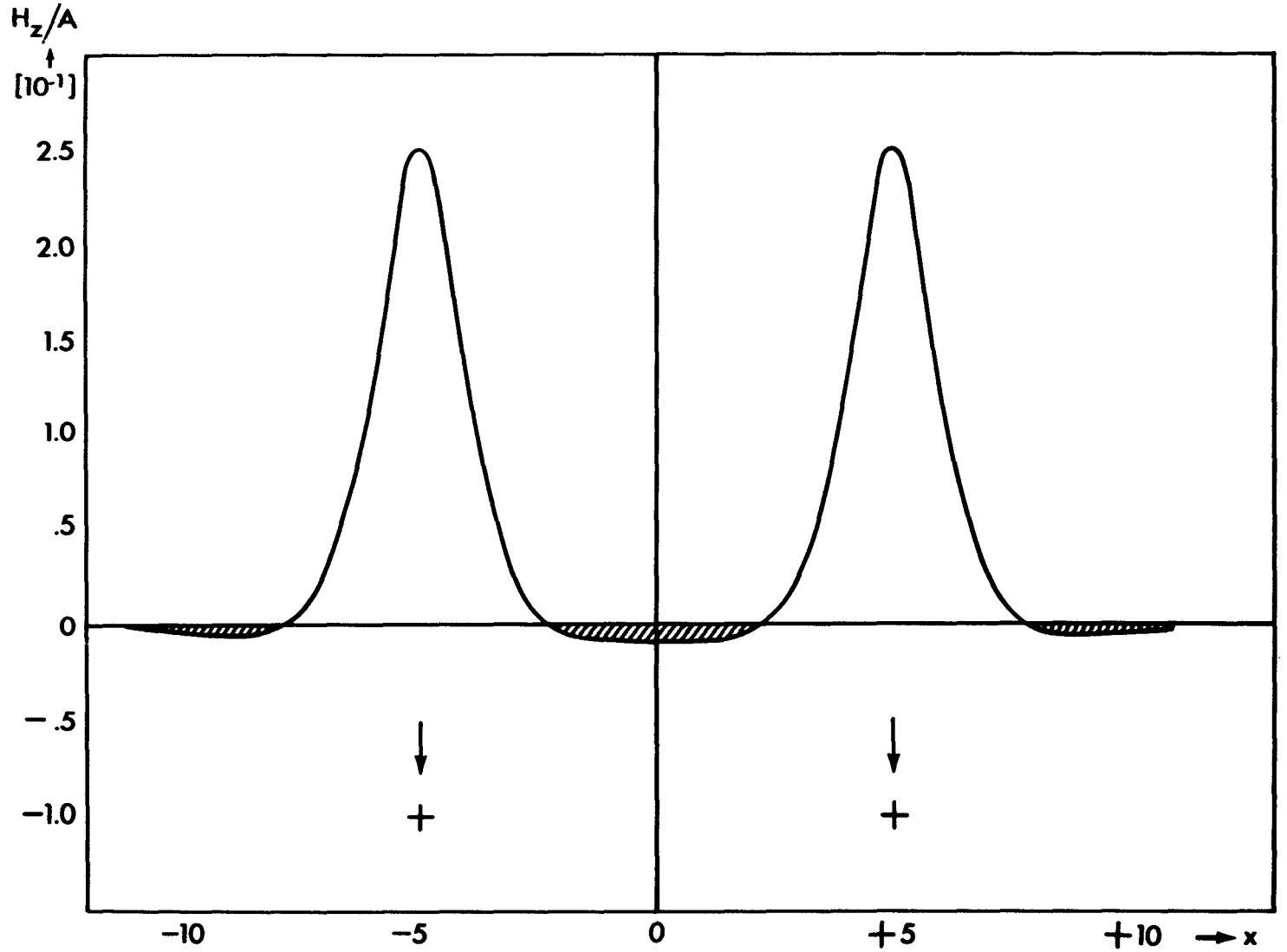

Fig. 21. H_z/A at z = 2 for two positive poles at x = +5 and -5.

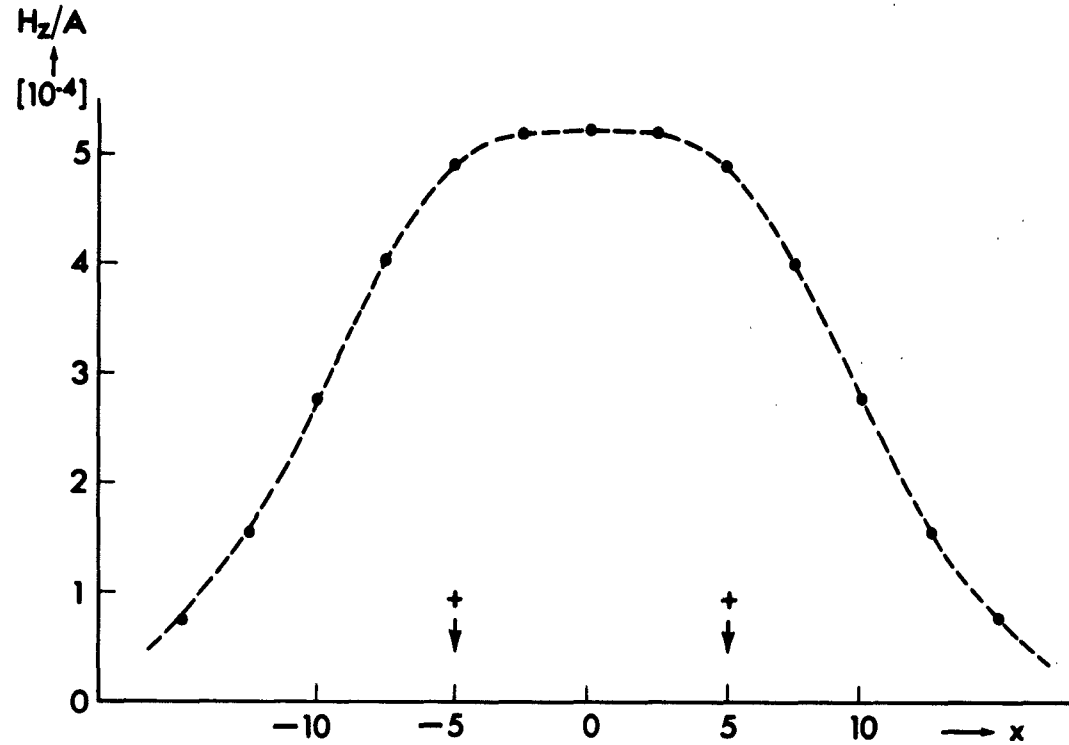

Fig. 22. H_z/A at z = 12.5 for two positive poles at x = +5 and -5.

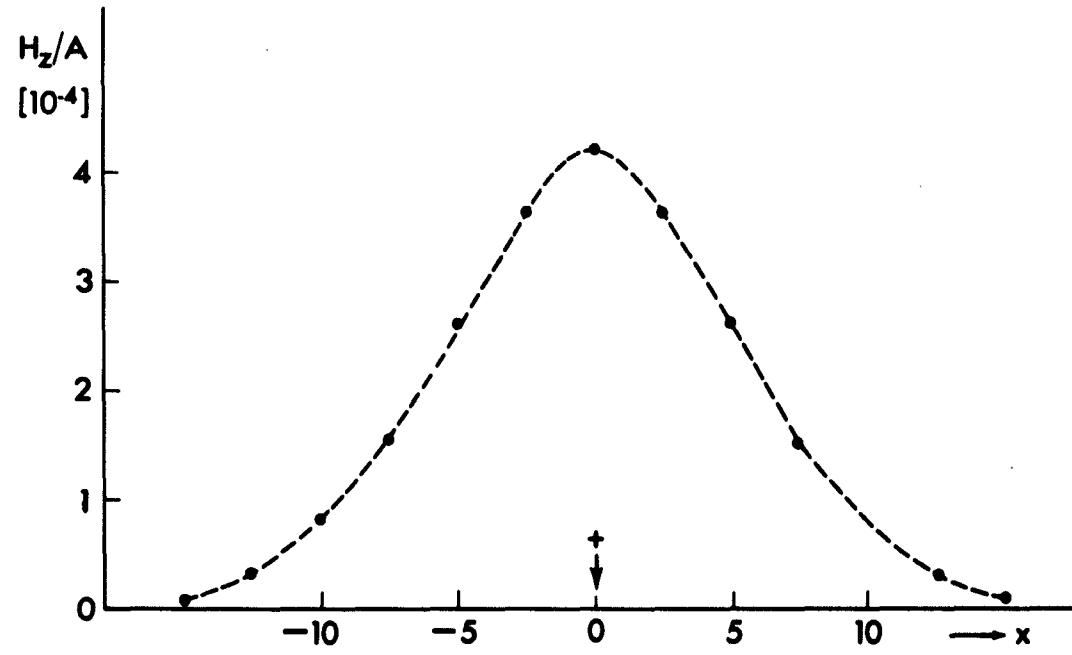

Fig. 23. H_z/A at z = 12.5 for a positive pole at x = 0.

Eq. (126) is identically satisfied for all values of z if x = 0. This point corresponds to the minimum. The general solution cannot be obtained in closed form; however, we see that a maximum occurs at

$$x = \pm d \qquad \text{if} \qquad z = d \,, \tag{127}$$

whereas a maximum occurs at

$$x = \pm d/2 \qquad \text{if} \qquad z = 5d/\sqrt{2} = 3.55\ d \,. \tag{128}$$

This behavior is schematically shown in Fig. 24.

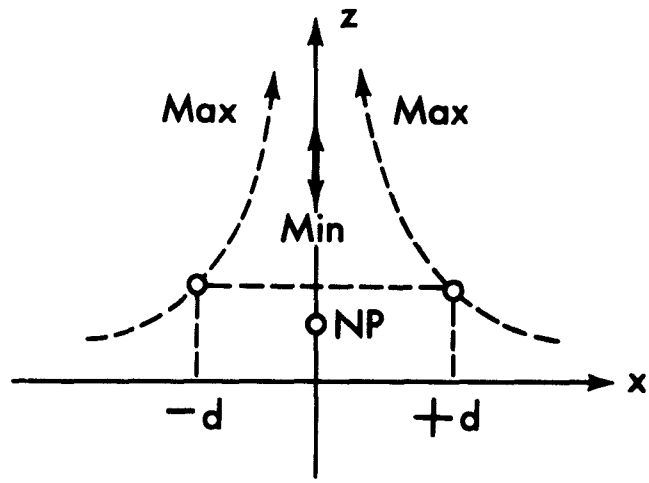

Fig. 24. Positions of maxima of H_z for equal poles at x = +d and -d.

Not at all considered is a difference in height of the generating current loops, since this effect can certainly not be deduced from Michard's observations.

Turning now to the difference between spot locations and positions of field maxima, we note that on April 23 the inclination of the sun's rotational axis is about -5°.3, presenting the image shown in Fig. 25 to an observer on the earth. Because of the sun's inclination the effective angle between the line of sight and the EW-line is reduced to about 15°, whereas the angle between the NS-line and the line of sight is the full 25°. In the following, the effects of this inclination are studied, taking the average angle of 20° as a test case.

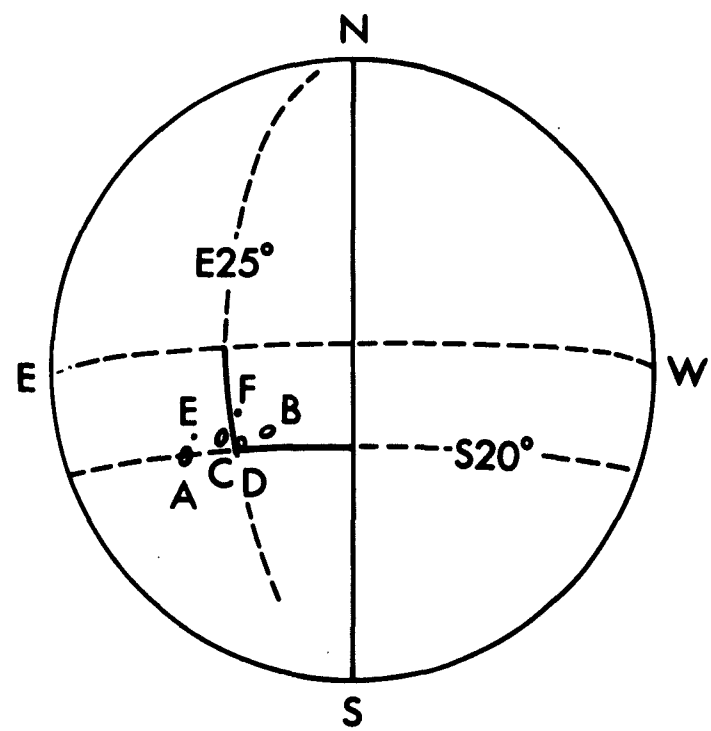

Fig. 25. Position of spot group on the sun, April 23, 1960. (Michard et. al., 1961)

We restrict this model calculation to the plane y = 0, and then need only the components H_x and H_z. Taking the two cases described previously (Figs. 22 and 23) and plotting field amplitude and direction, we obtain the field components in the line of sight as given in Figs. 26 and 27. The schematic diagrams show the predicted field distribution around the quadrupole and around the single pole. The similarity to Fig. 19 is obvious: the relative shift for the quadrupole is considerably stronger than the shift for a single pole. Exactly this behavior was found under points (1) and (2), p. 50.

A continuation of this type of study with more observational material would be highly desirable, since it cannot be ruled out that the rather encouraging results of this section are fortuitous. A study of the magnetic field distribution as reflected by different lines, originating in different levels of the photosphere or chromosphere, would add direct observational evidence for the height variation of the fields. The great difficulties of the field measurements make it probably unpractical to look for statistically significant variations in field strength. However, it may be possible to study the relative frequency of "irregular" regions of opposite polarity. Since we believe that many field measurements refer to layers very close to NP's, a small variation in effective height may result in considerable changes, in particular around "irregular" regions.

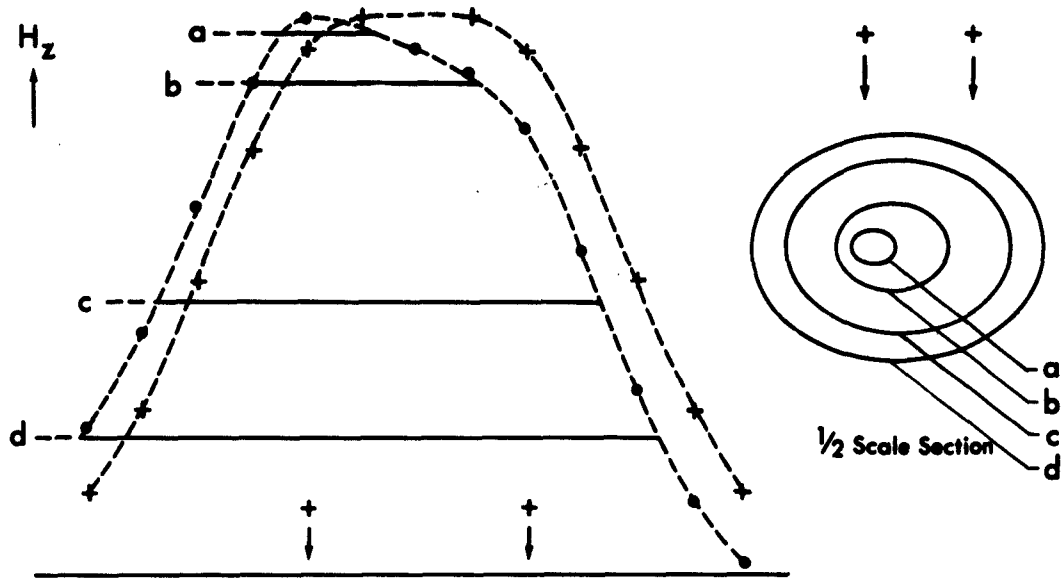

Fig. 26. Modification of Fig. 22 for inclined line of sight. Two equal poles on x-axis.

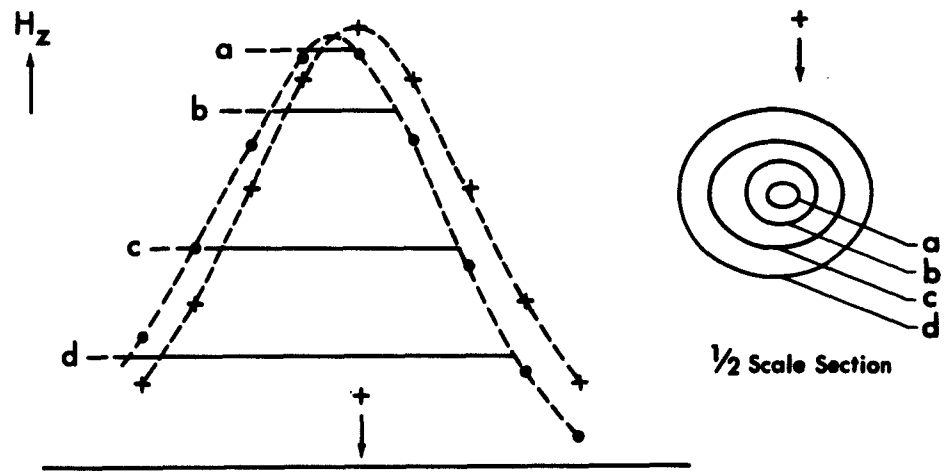

Fig. 27. Modification of Fig. 23 for inclined line of sight. Single pole on x-axis.

With the relatively simple, but apparently rather powerful mathematical model developed in the first sections, it should be possible to predict the approximate position (and height) of NP's in spot groups of known geometry more accurately than is possible with the qualitative methods employed previously. On this basis it may be possible to come to some conclusions as to the correlation between NP's and points of origin of flares.

11. LOCAL FIELDS IN THE CORONA

All considerations on which we elaborated in the preceding sections assumed that no electric currents flow above subphotospheric regions. This is certainly not quite correct, as has been pointed out already by Gold (1958). The reason is that force-free fields in the outer corona can never produce the observed departures of the density distribution from hydrostatic equilibrium. If these structures are tied in with magnetic fields, the fields must deviate more or less from the force-free type. Since the density increase is stable over relatively long periods of time, it must be accompanied by magnetic fields which hold it in place, and these fields originate

in local electric currents in the corona.

The problem can therefore be put in the form of asking what kind of local magnetic field would be required to produce a stable density distribution of the type observed, for instance, in coronal streamers.

A complete and correct answer to this question involves prohibitively complex mathematics and is therefore far beyond the scope of this report. A few general theoretical remarks will be added in an Appendix. We prefer to advance in the remainder of this section a suggestion as to a possible starting point for local fields due to the underlying, admittedly force-free, field of the spot group. In order to keep in close contact with observed features, we summarize briefly the relevant features of the enhanced radio radiation of the slowly varying type.

Solar disturbances ("Centers of Activity") emit above 600 Mc/s a type of radio radiation which is almost certainly thermal in origin (i.e. bremsstrahlung), and whose intensity is markedly above the background radiation of the chromosphere and lower corona. The increase in brightness temperature is due to the fact that regions above the chromosphere contribute an appreciable amount to the total radiation. Since the observed radiation temperatures (emitted intensity per unit area on the sun equated to a Planck function and expressed through

Rayleigh-Jeans' law in the form of temperatures) are in general well below the kinetic temperature of the undisturbed corona, i.e., approximately 2×10^6°K, it is generally assumed that the emitting regions are optically thin, or at least not completely opaque. The uncertainty in the calibration as well as the difficulties encountered in unfolding the interferometer pattern, however, make an accurate estimate of the optical depths involved at present impossible. For a detailed discussion see Newkirk (1961).

The contribution of the coronal rays above solar disturbances, i.e., the "activity centers" connected with sunspots, can be either attributed to a local increase in kinetic temperature (Waldmeier and Mueller, 1950), or to a locally increased density, possibly both. Newkirk has presented arguments in favor of an increase of the density alone. We shall follow his suggestion.

The correlation between the occurrence of the Slowly Varying Component (SVC) and the plage area surrounding the sunspot group is very good, in particular at higher frequencies, and better than with any other phenomenon of the centers of activity. It is therefore generally concluded that the SVC originates in coronal condensations above plage areas. There is an additional observation in favor of this concept, namely, the cosine-variation of the area emitting the SVC as a function of position on

the sun. The obvious interpretation of this observation is to assume a disk-like shape for the emitting region.

The postulated similarity of the shape of plage areas and the sources of the SVC is not easily understood. They are, of course, not simply identical. In the first place, plage areas and faculae are photospheric and chromospheric phenomena with no observed correspondence in the coronal behavior. It would therefore appear that postulating disklike structures in the corona requires a separate explanation, in the sense, that the flatness of the SVC source must be understood in terms of a physical theory, whereas this structure is rather trivial in the case of the essentially plane plages: while the plage area (being chromospheric in origin) is limited to a thin shell-type medium, the source of the SVC is embedded in the corona whose geometry is decidedly three-dimensional. Secondly, the statistical correlation between the horizontal extent of the sources and the plage areas does not necessarily point to any direct physical connection, but merely suggests that the source of the SVC is larger than the spot group to which it is connected. The same is true for the longevity of both the plage and the SVC source. On the other hand, there is no counterpart in the behavior of plages to the daily changes observed in the SVC, as described for instance in the radio heliograms (1420 Mc, Sydney), published in Vol. XXII of the Annals of the IGY.

We shall suggest that the source of the SVC is due to the magnetic field configuration above sunspot groups and even between adjacent groups. A good example of this latter type is furnished by the chain of spots in the N-hemisphere on December 22 and 23, 1957. Whereas no other phenomenon has apparently undergone significant changes, except maybe the magnetic polarities not yet published, the SVC source changed from a doubly-peaked shape, with the maximum between the two major groups. The spatial resolution of the antenna is considerably better than the quoted details (half-power points approximately 3° in both coordinates).

It may be argued that the relatively weak polarization of the SVC speaks against a dominant influence of the magnetic fields. We shall presently show, however, that the source of the SVC in our concept is situated at the minimum of the magnetic field and, moreover, in a rather complicated field structure which would make a uniform polarization rather unlikely.

In order to investigate this suggestion in some detail, we consider as a typical example the set of two plane quadrupoles, discussed in Section 6. Offhand, this model is best suited to represent two separate spot groups, whereas the majority of strong SVC sources lie above bipolar groups. In the latter cases a very complex field structure close to the chromosphere, in general with several NP's, can be expected. The regions around these NP's would then be the place of the source of the SVC, in

the manner outlined below for the two quadrupoles. The NP's above single groups are of course at a lower height, hence in regions with higher density and lower kinetic temperature. From theory alone, it is impossible to predict offhand whether the combination of these two qualities on the average leads to a higher or lower value of the brightness temperature as compared with a source above two spot groups. Statistical investigations of this point are clearly needed.

The magnetic field of the two combined quadrupoles reads

$$H_x = 2Ad \cdot 3z \left\{ \frac{1}{r_+^5} + \frac{1}{r_-^5} - 5\left[\frac{(x + D)^2}{r_+^7} + \frac{(x - D)^2}{r_-^7} \right] \right\} \tag{129}$$

$$H_y = - 2Ad \cdot 15yz \left\{ \frac{x + D}{r_+^7} + \frac{x - D}{r_-^7} \right\} \tag{130}$$

$$H_z = - 2Ad \left\{ \frac{x + D}{r_+^5} \left[2 + \frac{5}{r_+^2} (2z^2 - y^2 - (x + D)^2) \right] \right.$$

$$\left. + \frac{x - D}{r_-^5} \left[2 + \frac{5}{r_-^2} (2z^2 - y^2 - (x - D)^2) \right] \right\} \tag{131}$$

with

$$r_+^2 = (x + D)^2 + y^2 + z^2, \quad r_-^2 = (x - D)^2 + y^2 + z^2 . \tag{132}$$

It is assumed that the field is computed in the far-zone of each individual quadrupole, but not of the system (cf. Section 6). The direction of the field is the same for both quadrupoles, situated on the x-axis at $x = \pm D$.

Some of the properties of this system have been discussed previously (Fig. 9). For instance, there is a NP in the plane of symmetry $x = y = 0$ at $z = 2D$ [Eq. (72)]. It is interesting to note that the height of this NP is considerably less, if the assumption $D >> d$ (Eq.[67)] is dropped. As an example, we quote the height of the NP

$$z = 1.84\ D \tag{133}$$

for an arrangement of single poles as illustrated in Fig. 28.

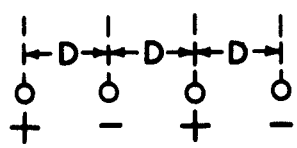

Fig. 28. Arrangement of single poles producing a NP at $z = 1.84\ D$.

In the plane y = 0, the field has schematically the form shown in Fig. 29.

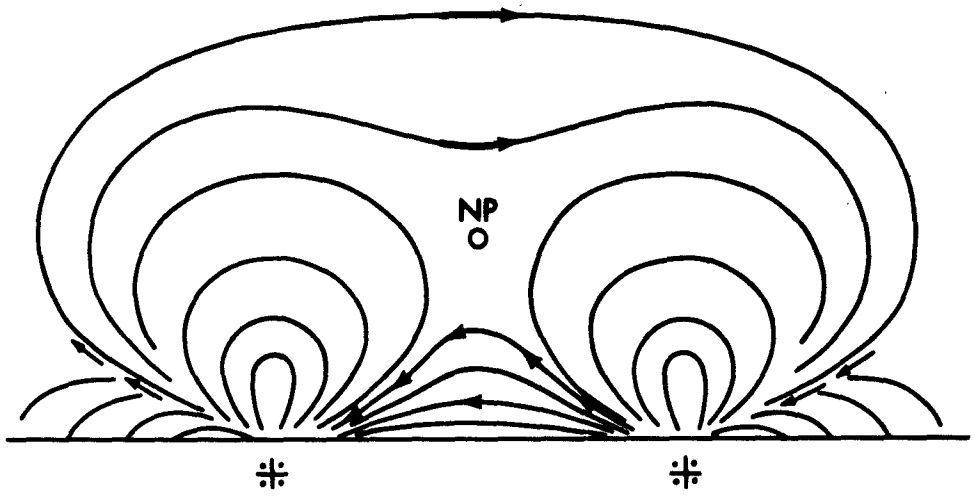

Fig. 29. Field of two combined quadrupoles in the plane y = 0.

We have carried out numerical calculations for the case D = 10, and plotted in Fig. 30 the square of the total field strength in units of 2Ad in the plane y = 0:

$$\beta^2 = \beta_x^2 + \beta_z^2 = \frac{H^2}{4A^2d^2} \; ; \quad \beta_y^2 = 0 \; . \tag{134}$$

The remarkable feature of Fig. 30 is the region of low field-strength in the neighborhood of the NP. Clearly, charged particles will be trapped at that location in much the same manner as in a mirror geometry in thermofusion experiments.

The calculations on which Fig. 30 is based concern strictly force-free fields. Due to the trapping, however, the density at the NP must increase, leading to local coronal fields which will certainly change the field structure. Intuitively, one would expect the net result to be an expansion of the low field region, hence, an increase of the excess electron (and ion) density in the neighborhood of the NP. A steady state will be reached in the zone of confinement when diffusion across the field lines equals the number of particles flowing in.

It is very suggestive to hypothesize that a change in the general field structure may compress the region of confinement, resulting in an increase in kinetic temperature to points at which thermo-nuclear reactions begin. This point of view has been stressed several times by Severny as a possible cause for solar flares. The main argument against this idea is the absence of strong changes in the photospheric magnetic field structure during and probably even before the onset of flares. We believe that no such drastic changes would be required in the geometry considered here (and qualitatively as well by Severny). It should be mentioned though that so far attempts to locate sizable quantities of deuterium in solar flares have failed.

There is a simple source for the postulated particle inflow. Extending the field model in the plane $x = 0$ to finite values

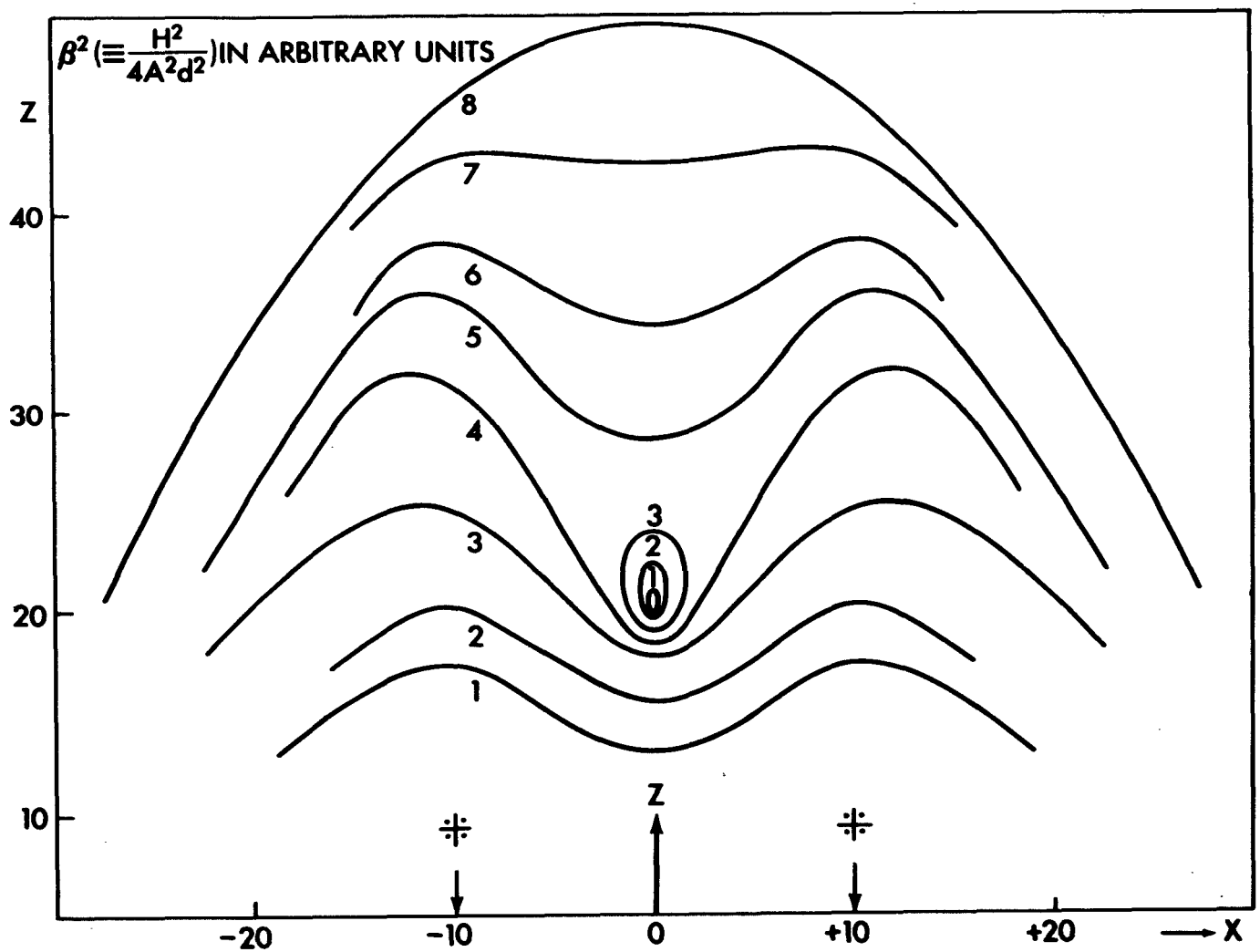

Fig. 30. Square of the total field strength (in units of 2 Ad) in the plane y = 0 for two combined quadrupoles at x = +D and -D, for D = 10.

of y, we find that the NP of Eq. (72) really is the intersection of a one-dimensional "NEUTRAL LINE", along which the total field strength vanishes with the plane y = 0. In fact, it is easy to see from Eqs. (129) - (131) that for

$$x = 0: \quad H_y = H_z = 0 \tag{135}$$

whereas

$$H_x = 2Ad \cdot 6z \left[\frac{1}{(D^2 + y^2 + z^2)^{5/2}} - \frac{5D^2}{(D^2 + y^2 + z^2)^{7/2}} \right] . \tag{136}$$

H_x vanishes for all

$$z^2 = 4D^2 - y^2 . \tag{137}$$

The Neutral Line touches the plane z = 0 for

$$y = 2D . \tag{138}$$

A schematic picture of the quantity β^2 in the plane x = 0 is given in Fig. 31.

We see that the region of small field intensity lies in the symmetry plane of the two quadrupoles, reaching a maximum height of 2D, and arching back to the photosphere at y = ± 2D. It is suggested that from the photosphere and chromosphere the particles enter the region of confinement. It is conceivable that the higher density of the chromosphere is maintained throughout this region, thus causing the coronal condensation responsible

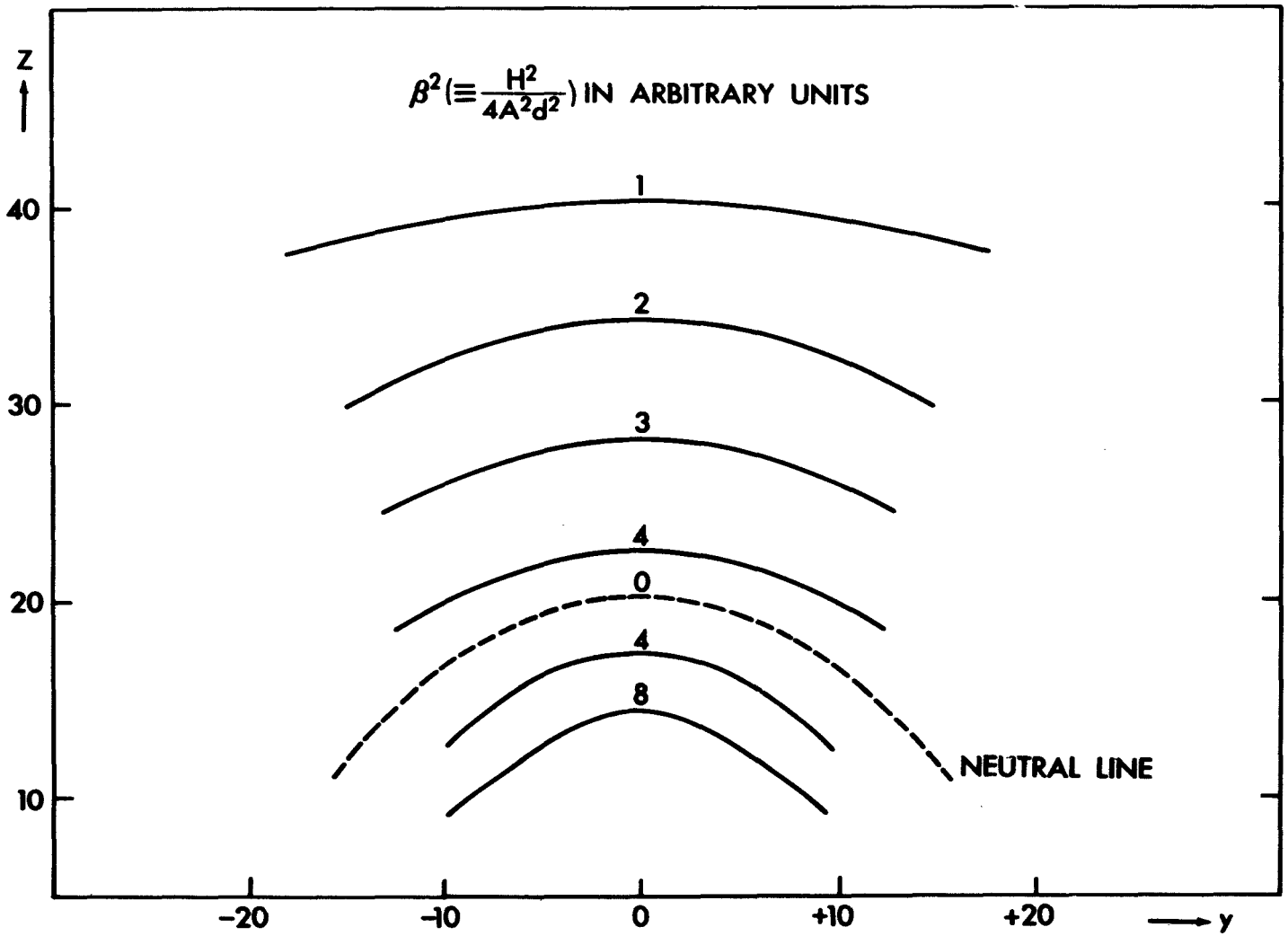

Fig. 31. Square of the total field strength (in units of 2 Ad) in the plane x = 0 for two combined quadrupoles at x = +D and -D, for D = 10. Note neutral line.

for the SVC.

With an assumed separation of 10° between two spot groups on the sun, we find the NP at approximately 100 000 km height. This value is quite reasonable if one recalls that in an actual case the field of two spot groups at the NP is not yet in the far zone, resulting in an effectively lower value for the height of the NP.

An additional consequence of interest of this hypothesis is that one would expect the source of the SVC to be on the average elongated in the direction approximately perpendicular to the equator. The radio heliograms published in the Annals of the IGY seem to support, at least qualitatively, this conclusion. A statistical analysis of the data seems possible.

APPENDIX

LOCAL FIELDS AND CURRENTS IN THE CORONA

In Section 11 the problem of deriving local magnetic fields in the corona from a (supposedly) known density distribution was mentioned, and it was stated that for mathematical reasons detailed calculations are beyond the scope of this report. We would like to clarify this point by considering the general set of electromagnetic equations relevant to the problem.

Assuming a steady state, ($\partial/\partial t = 0$) we have from Maxwell's equations

$$c\,(\nabla \times \vec{H}) = 4\pi\,\vec{j}\,, \tag{139}$$

and from the equation of motion

$$\frac{1}{c}\vec{j} \times \vec{H} = \nabla p + \rho \cdot \nabla \Phi\,. \tag{140}$$

Eliminating $\vec{j}$ leads to

$$\vec{H} \times (\nabla \times \vec{H}) = -\,4\pi\,\nabla p + 4\pi\vec{g}\,\rho\,. \tag{141}$$

$\vec{H}$ is the total magnetic field at any point in the corona, $\vec{j}$ the specific current in e.s.CGS units, p the pressure, Φ the gravitational potential, $\vec{g}$ the gravitational acceleration (in direction of the negative z-axis), ρ the matter density. The general equations and the physical characteristics of the quantities are discussed by Spitzer (1956), p. 20.

We split the magnetic field into a force-free part due to subphotospheric currents $\vec{H}^{o}$ and a local coronal field $\vec{H}^{*}$, so that

$$\vec{H} = \vec{H}^{o} + \vec{H}^{*}, \quad \nabla \times \vec{H}^{o} = 0, \quad \nabla \times \vec{H}^{*} \neq 0 , \tag{142}$$

and

$$\nabla \cdot \vec{H}^{o} = \nabla \cdot \vec{H}^{*} = 0 \tag{143}$$

everywhere.

Since

$$p = N_t \, KT \tag{144}$$

(N_t is the total number of particles, T the temperature, I Boltzmann's constant), we have for an isothermal corona

$$\nabla p = KT \cdot \nabla N_t . \tag{145}$$

Under coronal conditions (complete ionization, 0.85 hydrogen, 0.15 helium in atomic numbers)

$$p = 1.87 \, NKT, \tag{146}$$

where N is the number density of electrons, and

$$\rho = 0.87 m_H N, \tag{147}$$

where m_H is the mass of the proton.

Splitting again p and ρ and, thus, N into a part N° referring to the "undisturbed corona" and a part N* referring to the additional density in the condensation, we have

$$\nabla p^{\circ} - \rho^{\circ} \vec{g} = 0 \ , \tag{148}$$

so that

$$- \nabla p + \rho \vec{g} = - 1.87KT \ \nabla N^{*} + 0.87 m_{H} \vec{g} \ N^{*} \ . \tag{149}$$

Retaining p and ρ for brevity, we have instead of Eq. (141)

$$\vec{H} \times (\nabla \times \vec{H}) = \vec{A} \ , \tag{150}$$

where

$$\vec{A} = - 4\pi \ \nabla p^{*} + 4\pi \vec{g} \ \rho^{*} \ . \tag{151}$$

are treated as known functions.

If $\nabla \times \vec{H} \perp \vec{H}$,

$$\vec{H} \cdot (\nabla \times \vec{H}) = 0 \ . \tag{152}$$

The vector system of equations (150) - (152) has the solution (Madelung 1957)

$$\nabla \times \vec{H} = \nabla \times \vec{H}^{*} = - \frac{\vec{H} \times \vec{A}}{(\vec{H})^{2}} \ . \tag{153}$$

Condition (152) means that the magnetic field is perpendicular to the electric currents, i.e., that any current component parallel to the magnetic field is neglected. Such a

component would, of course, not be affected by the field. Hence no immediate difficulties arise from the use of Eqs. (152) and (153).

Eq. (153) represents an integral equation in vector form which hardly can be solved with any reasonable amount of effort. We tentatively linearize the system by postulating that

$$\vec{H}^{\circ} >> \vec{H}^{*} \tag{154}$$

which brings Eq. (154) into the form

$$\nabla \times \vec{H}^{*} = - \frac{\vec{H}^{\circ} \times \vec{A}}{(\vec{H}^{\circ})^2} = \vec{C} . \tag{155}$$

Because of Eq. (143), Eq. (155) represents the well-known problem of a vector potential and has the solution

$$\vec{H}^{*} = \frac{1}{4\pi} \nabla \times \int \frac{\vec{C}}{|\vec{r} - \vec{r}'|} dV , \tag{156}$$

where $\vec{r}'$ is the radius vector to the observer's point to which the vector ∇ refers, $\vec{r}$ is the radius vector to the field point which is the subject of the integration over all space.

For the linearized form, Eq. (152) is not self-evident any more. As a matter of fact, it now has the significance of a restriction of the physical situation which ought to be justified for each case separately, i.e., for each pair of

vectors $\vec{H}^o$ and $\vec{C}$. A solution of this difficulty will be suggested below.

Eq. (156) can be written in a slightly less cumbersome form by carrying out the curl-operation. Noting that the ∇ - vector operates only on the radius vector $\vec{r}'$ in the denominator, we find that

$$H^* = \frac{1}{4\pi} \int (\vec{r} - \vec{r}') \times \frac{\vec{H}^o \times \vec{A}}{(\vec{H}^o)^2} \frac{dV}{|\vec{r} - \vec{r}'|^3} . \qquad (157)$$

Writing Eq. (157) in more detail, one has to solve

$$H^* = \int \frac{(\vec{r} - \vec{r}')}{(H^o)^2} \left[\vec{H}^o \times \left(\nabla p^* - \vec{g} \rho^* \right) \right] \frac{dV}{|\vec{r} - \vec{r}'|} , \qquad (158)$$

For $\vec{H}^o$ one may substitute any of the fields discussed in the preceding sections, preferably the field of a bipolar group (quadrupole field) of Eqs. (42) to (44).

For a given density distribution, Eq. (158) leads to a field which is strictly of coronal origin. One could now think of starting an iteration procedure, introducing the field $\vec{H}^o + \vec{H}^*$ on the right-hand side of Eq. (160), thus obtaining a new solution $\vec{H}^1$, etc. If the procedure converges, the final correct solution would automatically fulfill condition (152).

Without going into tedious numerical calculations it is not obvious in what direction the coronal field $\vec{H}^*$ and the following iteration products would alter the force-free field $\vec{H}^o$. The method itself, however, seems sufficiently interesting to be mentioned.

CONCLUSIONS

1. It is shown that a model ascribing the magnetic field of sunspots to subphotospheric currents, idealized by loop currents underneath each spot, leads to a satisfactory representation of observational data on photospheric layers. For all practical purposes, the field expressions in the far-zone approximation are sufficient and which for a single sunspot are identical with the field of a dipole whose axis is perpendicular to the solar surface.

2. The field of the simplest bipolar group consisting of two single spots of opposite polarity is of quadrupole character in the far-zone, i.e., the total field strength varies as the minus fourth power of the radial distance. Field lines in the upper half-plane arrange themselves in a cone of 90° aperture, provided the pole strengths of the two major spots are equal. If the pole strengths differ, the field becomes asymmetric, resulting in an inclination toward the weaker pole. The angle of inclination with respect to the normal direction is approximately 55° at great distance, and is independent of the relative pole strength. Only the height level at which this inclination is effectively reached depends on the relative pole strength.

3. If more than one spot of the same polarity is present

in a group, neutral points of vanishing total field strength occur. The height of such a neutral point depends on a variety of parameters, notably, spot radii, distances between spots, relative pole strengths, etc. In most simple cases, however, the height counted from the plane of the current loops is of the same order as the distance between the spots, thus being very sensitive to small changes in the position of spots. The same conclusion can be drawn from more complicated field geometries due to three or more spots.

4. A detailed comparison of photospheric measurements by Michard et al., loc. cit., with our model shows that all major observed features are at least qualitatively represented by the model. It follows that a model making use of force-free fields in photospheric layers does not lead to grave errors, and might therefore be extended with a fair chance of success to predict fields in the outer atmosphere, notably the corona. One obvious application of this principle is the direct calculation of occurrence and height of neutral points for actual spot geometries.

5. It is anticipated that the density in the neighborhood of neutral points is strongly increased due to the trapping of charged particles. From our model calculations follows indeed

a mechanism for feeding particles into the region of confinement. It is admitted, however, that local non-forcefree currents will probably play a dominant role in the steady state maintenance of these coronal condensations.

REFERENCES

Babcock, H. W., and H. D. Babcock, IAU Symposium No. 6, Stockholm 1956, 239, Ed. Lehnert, (1958), (see in particular Plate II).

Blewett, J. P., J. Appl. Physics, 18, 968, (1947).

Bruzek, A., Z.f. Astrophysik 44, 183, (1958).

Bruzek, A., Z.f. Astrophysik 50, 110, (1960).

Bumba, V., Izv. Krymsk. Astr. Obs., 19, 105, (1958).

Cowling, T. G., Solar Electrodynamics, "The Sun", Ed. G. P. Kuiper, 583-590, (1953).

Dungey, J. W., IAU Symposium No. 6, Stockholm 1956, 141, Ed. Lehnert, (1958).

Dwight, H. B., Tables of Integrals and Other Mathematical Data, MacMillan Co., 3rd Ed., 171, (1957).

Evans, John W., The Astronomical Journal, 64, 330, (October 1959).

Giovanelli, R. G., Monthly Notices R.A.S., 107, 338 (1947).

Giovanelli, R. G., Monthly Notices R. A. S., 108, 163 (1948).

Glasstone and Lovberg, Controlled Thermonuclear Reactions, Van Nostrand: Princeton, N. W., 130, (1960).

Gold, T., IAU Symposium No. 6, Stockholm 1956, 275, (1958).

Grotrian, W., and H. Künsel, Z.F. Astrophysik, 28, 28, (1950).

Howard, R., T. Cragg, and H. W. Babcock, Nature 184, 351, (1959).

Hoyle, F., Some Recent Researches in Solar Physics, Cambridge: University Press (1949).

Madelung, E., Die Mathematischen Hilfsmittel des Physikers, 6th Ed. 1957, 233, Springer Verlag, Heidelberg.

Michard, R., Z. Mouradian, and M. Semel, Annales d'Astr., 24, 54, (1961).

Newkirk, G., Ap. J., 133, 983, (1961).

Noyes, J. C., Boeing Document D1-82-0189, (June 1962).

Obayashi, T., and Y. Hakura, J. Geophys. Res., 65, 3143-3148, (October 1960).

Severny, A. B., Izv. Krymsk. Astr. Obs., 20, 22, (1958).

Severny, A. B., Izv. Krymsk. Astr. Obs., 22, 12, (1960).

Stepanov, V. E., Izv. Krymsk. Astr. Obs., 23, 184, (1960).

Stratton, J. A., Electromagnetic Theory., McGraw-Hill Book Co., New York, 263, (1941).

Spitzer, L., Physics of Fully Ionized Gases, Interscience Publ., New York, (1956).

Sweet, P. A., IAU Symposium No. 6, Stockholm 1956, 123, (1958).

van de Hulst, H. C., IAU Symposium No. 6, Stockholm 1956, 280, (1958).

Waldmeier, M., and H. Mueller, Z.f. Astrophysik, 27, 58, (1950).